Settling Dynamics of Spherical Particles in Fracking Fluids

Undergraduate Research Thesis

Presented in Partial Fulfillment of the Requirements for graduation "with Honors Research Distinction in Chemical and Biomolecular Engineering" in the undergraduate colleges of The Ohio State University

Ziwei Wang

The Ohio State University

2016

Project Advisor: Professor Kurt Koelling

Committee: Prof. Kurt Koelling and Prof. Isamu Kusaka

Abstract

Hydraulic fracturing is an enhanced oil and gas recovery method that involves pumping fluids and proppants into shale fractures. Fracking fluid is formulated to keep proppants suspended for a desired time. The flow of fracking fluid and the settling dynamics of proppants are of great interest in fracking wells. This research aims to add fiber suspensions to fracking fluid system to reduce the amount of chemical additives without compromising performance. In this research, fracking fluid samples are rheologically characterized, settling rates of rigid, dense spherical particles in fracking fluids are measured. Experimental conditions are reproduced using COMSOL Multiphysics. Simulation results are compared against experimental data and other modeling attempts.

The fracking fluid samples are homogenous mixtures of deionized water, 0.5 wt% guar, <0.1% sodium tetraborate and chopped fiber. Chopped fiber investigated nylon fiber with diameters of 25 and 38 microns and length of 6 and 10 millimeters and glass fiber with diameters of 50 microns and length of 3 and 6 millimeters. Fiber concentrations range from 0 to 15 nL^3, where n is number of fiber per milliliter of fracking fluid.

Results show that by fitting fracking fluids with Cross Model and using COMSOL laminar flow simulation, settling rates of proppants in fracking fluids can be accurately predicted. It is also observed both experimentally and computationally that addition of fiber reduces particle settling rate by more than 50%.

Acknowledgements

I would like to thank Dr. Kurt Koelling for his guidance and help throughout this project. I would also like to thank my group members Joseph Gauthier, Ann Maula, Tom Groseclose and Jack Jones who helped me in the lab. Finally, I would like to thank Dr. Isamu Kusaka for attending my thesis defense.

Vita

August 2012 - present.....B.S. Chemical and Biomolecular Engineering,

The Ohio State University

Table of Contents

List of Tables

List of Figures

1. Background and Motivation

This research investigates the settling dynamics of spherical particles in fiber-laden aqueous gel with applications in hydraulic fracturing. Hydraulic fracturing, commonly known as fracking, is a hydrocarbon capturing method to extract oil and gas in shale. It has been widely applied in US for natural gas production from unconventional reservoirs. Shown in Figure 1, it is accomplished by first drilling miles down into the crust to reach the reservoir, then use horizontal drilling technique to branch out within the field. After drilling, water is pumped into the well using high performance pumps, breaking the rock formation with tremendous pressure to free the trapped hydrocarbons. The pressure is then released to allow the hydrocarbons to flow up to the surface for collection [1]. One technical issue is that the newly formed fracture re-close upon the release of pressure and therefore reducing the yield. To maximize yield, special sand particles called proppants are delivered along with the water to keep the fractures open. Being more dense than water, proppants precipitates in water before being delivered underground[2]. To prevent settling, specialty fluids, also known as fracking fluids, are needed to suspend the proppant particles and transport proppant particles into fractures. In fracking wells, the fluid has to suspend and transport more than 10 volume percent proppant under high pressure and temperature for a desired time span. Typical fracking fluids are made from 99.5% water, 0.5% Guar as a viscosifier, <0.1% sodium tetraborate as a cross linker and other additives such as surfactants, biocides and corrosion inhibitors, etc. Figure 2 below shows the molecular structure of guar. It is a branched sugar chain polymer with molecular weight ranging from 10^5 to 10^6 . Sodium borate forms covalent bonds with the hydroxyl groups on the guar polymer and cross links the chains together, forming a network of molecular structure. The cross linking reaction is shown in Figure 3. Guar has minimal hazard to humans and the environment, as it is extracted from plants and is even used as thickener in food products. On the other hand, sodium tetraborate is considered a hazardous material[3]. To maximize the fluid's efficiency and reduce its impact on the Earth's environment, research is done to reduce the concentrations of chemical additives, specifically sodium tetraborate, without compromising performance. This research aims

to reduce cross-linker concentration by adding a small amount of chopped fiber to the fluid. [4] An optimal fiber choice would have a density close to water, have strong mechanical interactions with the fluid's crosslinked polymer molecule network to provide structural support and enhance the fluid's suspension capability without increasing fluid's viscosity or interacting with other components of the system.[4]

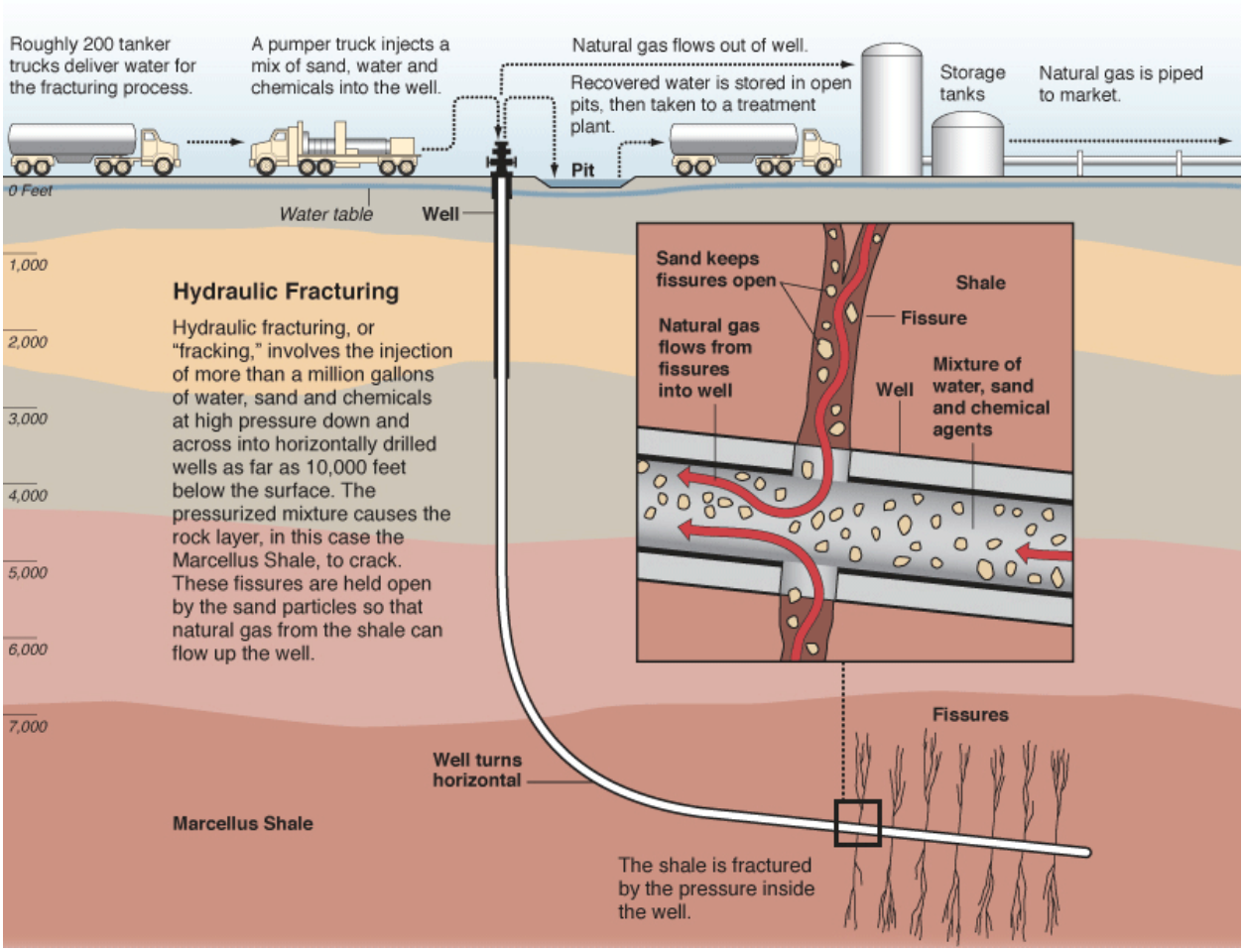

Figure 1 Hydraulic fracturing process[11]

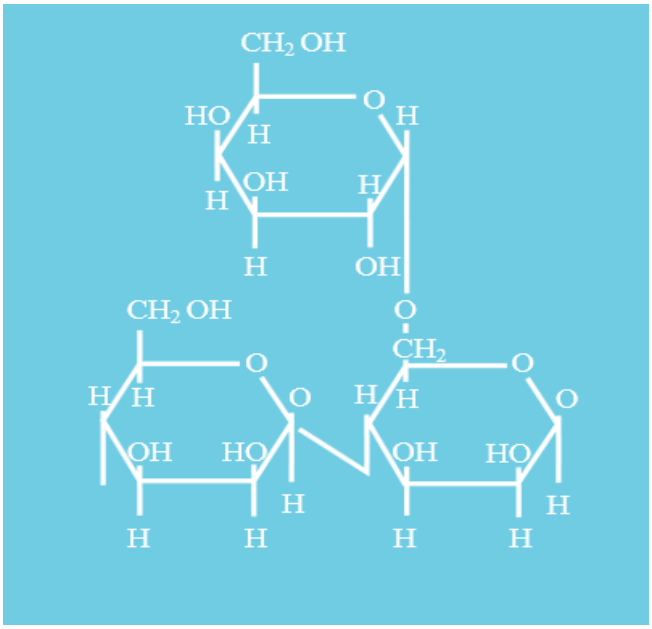

Figure 2 Molecular structure of guar[12]

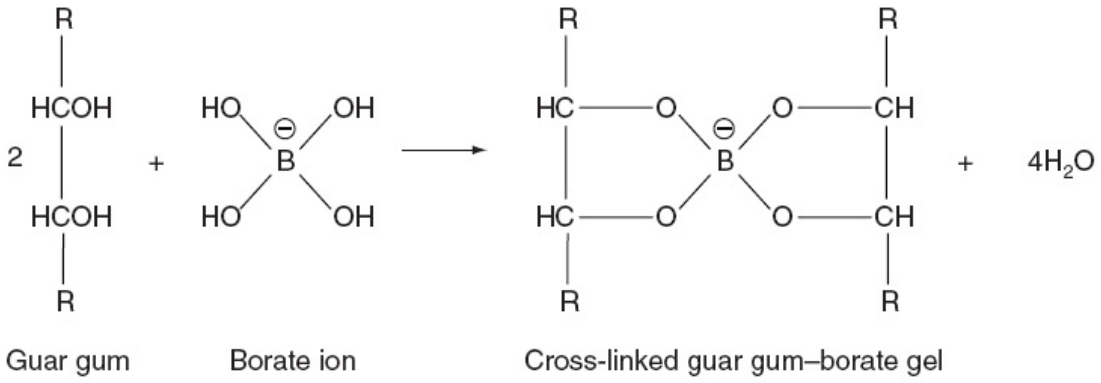

Figure 3 Crosslinking reaction between the guar backbone and the borate ion[13]

2. Literature Review

The fracking process can be simplified to a "spheres settling in fluids" model. Multiple models have been developed to predict settling rates of spheres in fluids. The simplest model is Stoke's Law of Settling, shown in Equation (1) below[6].

$$v_s = \frac{2}{9} * \frac{(\rho_p - \rho_f)}{\eta_0} * gR^2 \quad (1)$$

In this equation, ρ_p is the density of the particle, ρ_f is the density of the bulk fluid, g is the gravitational constant, R is the radius of the particle, and η_0 is the viscosity of the bulk fluid. This model assumes that the flow around the spherical particle is perfectly laminar (low Reynolds Number), the fluid is Newtonian, and a homogeneous bulk fluid.

Fracking fluid is a Non-Newtonian fluid. It is shear thinning and slightly elastic. The simplest Non-Newtonian model is Power Law, shown in Equation (2) below[7].

$$\eta_0 = k * \dot{\gamma}^{n-1} \quad (2)$$

In Equation (2), η_0 is the viscosity of the bulk fluid, $\dot{\gamma}$ is the shear rate, k and n are power-law parameters.

Graham and Jones [14] derived an empirical relation through computer simulation shown in Equation (1) below.

$$C_d = a(Re) + n * b(Re) \quad (3)$$

In this equation, n is the Power Law index. a(Re) and b(Re) are empirical functions of the particle Reynolds number Re. C_d is the drag coefficient, defined by Equation (4) below.

$$C_d = \frac{2 * F_d}{\rho_f * v^2 * A} \quad (4)$$

In this equation, F_d is the drag force on the particle, ρ_f is the fluid density, v is the velocity of the particle relative to the fluid and A is the projected area of the particle. Re, the Particle Reynold's number is defined by Equation (5) below.

$$Re = \frac{\rho_p * v * D}{\eta} \quad (5)$$

In this equation, ρ_p is the particle density, D is the particle diameter and η is the viscosity of the fluid.

When Reynold's number is smaller than 16 and greater than 0.2, which is slightly higher than the flow region of proppants settling in fracking fluids, the relation between drag coefficient and Reynold's number is shown in Equation (6) below.

$$C_d = \frac{35.2}{Re^{1.03}} + n * (1 - \frac{20.9}{Re^{1.11}}) \quad (6)$$

Clift, Grace and Weber [15] developed another empirical correlation between drag coefficient and particle Reynold's number for Reynold's number between 0.01 and 200, shown in Equation (7) below.

$$C_d = \frac{24}{Re} * [1 + 0.1315 * Re^{0.82-0.05*log_{10}Re}] \quad (7)$$

Recently, Shah, Fadili and Chhabra [16] developed a new model for spheres settling in Power Law Fluids shown in Equation (8) below. The new model is inspired by the fact that in empirical relations, both the drag coefficient has the velocity term in their expressions. By multiply the two quantities in such a way that velocity cancels, particle Reynold's number can be solved with just the power law parameters and the physical properties of the sphere.

$$\sqrt{{C_d}^{2-n} * Re^2} = A * Re^b \quad (8)$$

In this equation, A and b are empirical, quadratic functions of the power law index, n.

In summary, virtually all available studies concerning spheres settling in fluids are experimental or numerical. Analytical solutions of complex fluid problems are yet to be found.

3. Experimental methods

This research is carried out in three parts, rheological characterization, experimental settling rate measurements and COMSOL simulation and modeling.

3.1 Sample Preparation

Fracking fluid samples are prepared by blending 0.5 weight percent guar polymer into deionized water. The guar sample is obtained from Rhodia (JA Guar 418). Deionized water is measured into a blender. Guar polymer is added into the blender slowly as the solution is blended gently. The solution is blended for 30 seconds after addition of the polymer and is then transferred to a 500mL mason jar and is stirred with a magnetic stir bar at 300 RPM overnight to eliminate the bubbles. The samples are then divided into 100mL portions in 300mL mason jars. The crosslinker, sodium tetraborate, is measured and added to the samples. All samples are stirred with magnetic stir bars at 900 RPM till homogeneous. Chopped nylon fiber is added to samples and is stirred rigorously till the fiber is evenly dispersed by visual inspection.

3.2 Rheological Measurements

Rheological measurements are carried out with an ARES Rheometer, shown in Figure 4 below. Samples are measured with a 50mm parallel plate geometry, with a 0.5 mm gap. An dynamic oscillatory frequency sweep measurement (10% strain, 0.1 rad/s to 100 rad/s) and a steady rate sweep measurement (0.1 s^{-1} to 100 s^{-1}) is done for each sample.

Figure 4 ARES rheometer

3.3 Settling Rates Measurements

The fluid samples are transferred into 100mL graduated cylinders to conduct settling rate experiments. The settling rate experiments are conducted by dropping spherical particles into the fluid and measure the time it takes for the sphere to settle a certain distance. Measurements are taken after the particles reach steady state and are repeated and the average settling rate is recorded. The experiment setup is shown in Figure 5 below.

Figure 5 Experimental Setup

The spheres are acquired through McMaster Carr. The properties of the spheres are summarized in Table 1 below.

Table 1 Sphere Properties

	Density (g/mL)	Diameter (mm)
Glass Sphere	2.23	2.4
PTFE Sphere	2.2	1.6
Aluminum Sphere	2.7	1
Proppant	2	0.75

4. Results and Discussion

4.1 Rheology

In preliminary experiments, a batch of fluid sample is prepared for exploratory rheological testing. Figure 6, shown below, is a plot of shear viscosity vs shear rate for 0.5 wt% guar and 0.08 wt% sodium tetraborate fluid samples with different fiber concentration. It shows that the addition of chopped fiber to cross linked fluids has a negligible effect on the bulk fluid viscosity.

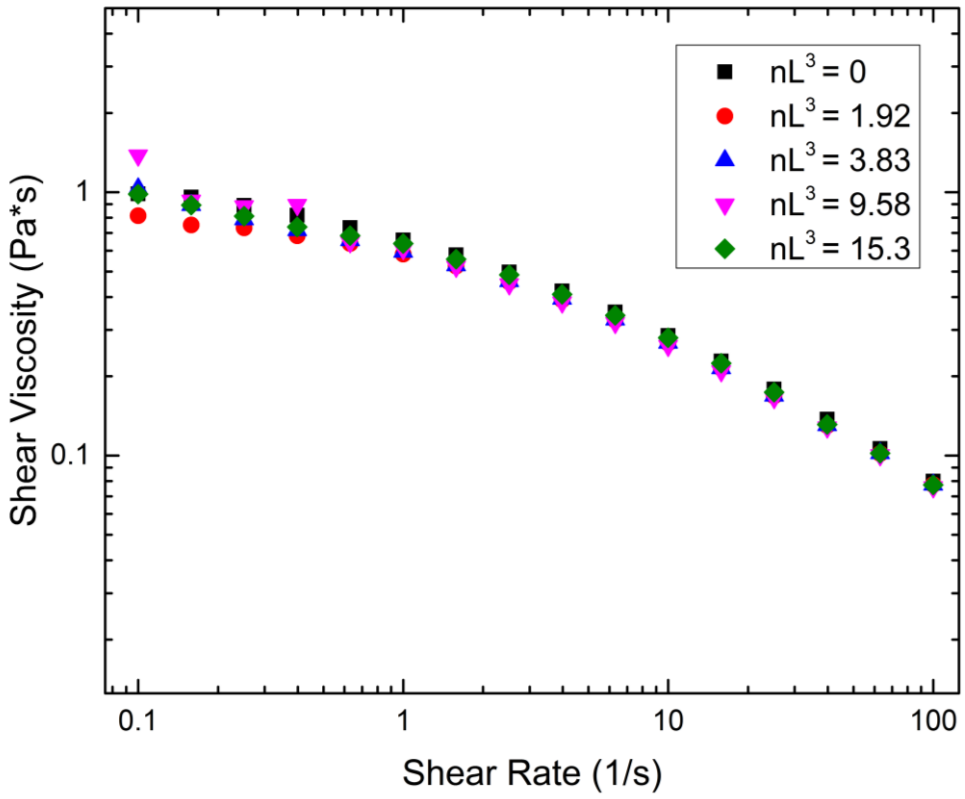

Figure 6: Ratio of bulk fluid viscosity containing fiber to fluid viscosity without fiber

With the fact that fiber has a negligible impact on rheological properties in mind, future rheological plots in this work will omit the fiber containing data, instead focusing on the experiments with fluids containing no fiber.

A strain sweep measurement is done to find the boundary of the linear viscoelastic region. Figure 7, shown below, depicts the results of the strain sweep data obtained at a frequency of 1 rad/sec, on the samples with different cross linker concentration. As can be seen, the rheometer is unable to resolve noiseless data at strains below 2% as a consequence of the rheometer being strain controlled. Because the torque signals from the fluid are low with low strains, noise as a result of friction in the rheometer and vibrations from the environment contribute significant portions of the signal. At strains higher than 2%, the torque from the fluid exceeds the noise signals. The plots show a clear increase in the elastic modulus with cross linker concentration, as expected since the cross linker links together polymer chains. Further, at strains between 40-100%, the elastic moduli at all cross linker concentrations begin to decrease, indicating that the fluid is approaching nonlinear region. With this in mind, all frequency sweeps were performed at a strain of 10% so that a strong torque signal could be achieved while staying in the linear viscoelastic regime.

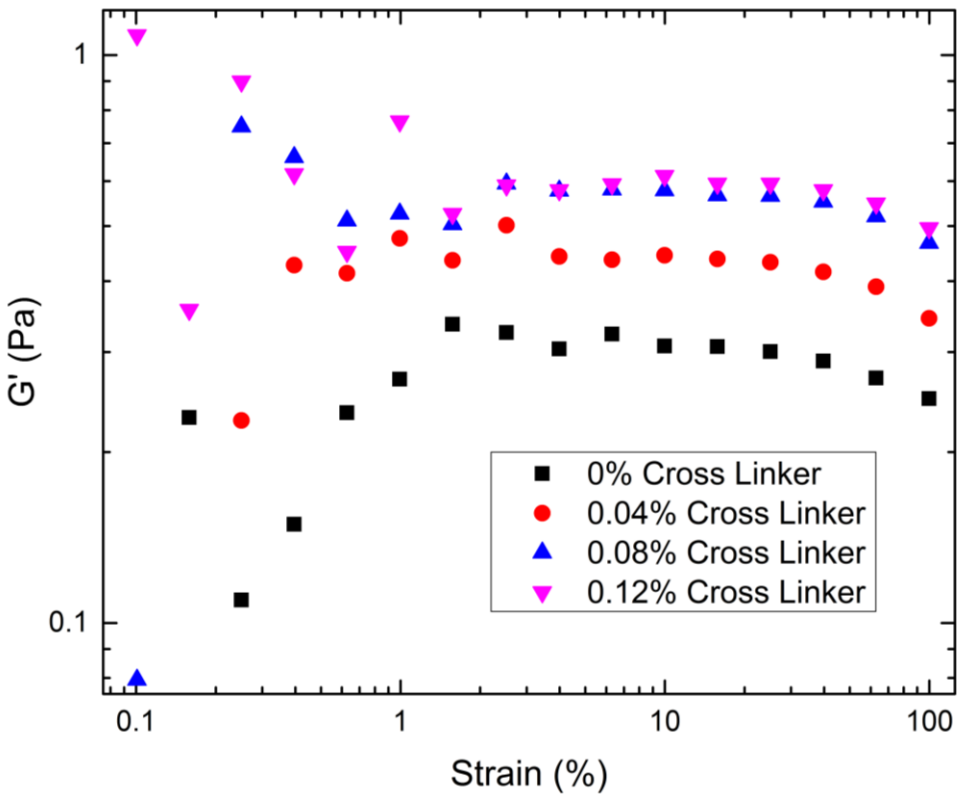

Figure 7: Strain Sweep Results

With the linear viscoelastic limit known, dynamic oscillatory experiments were performed on the fracking fluids to determine how G' and G'' vary with frequency and cross linker concentration.

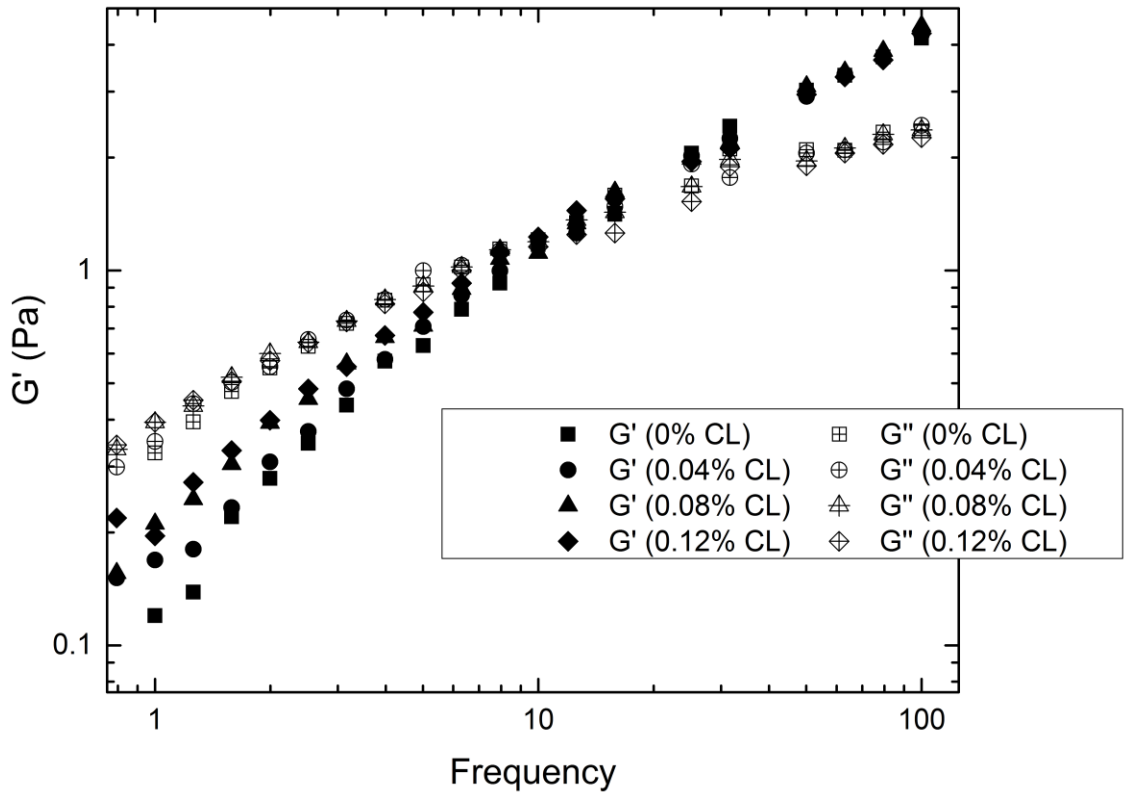

Figure 8: G' as a function of frequency, cross linker (CL) concentration

A complex viscosity can be defined as a geometric mean of G', G'' divided by frequency[7]. This definition is given by Equation (9), below. Further, a plot of complex viscosity as a function of frequency and cross linker concentration is given in Figure 9.

$$\eta^* = \sqrt{\left(\frac{G'}{\omega}\right)^2 + \left(\frac{G''}{\omega}\right)^2} \qquad (9)$$

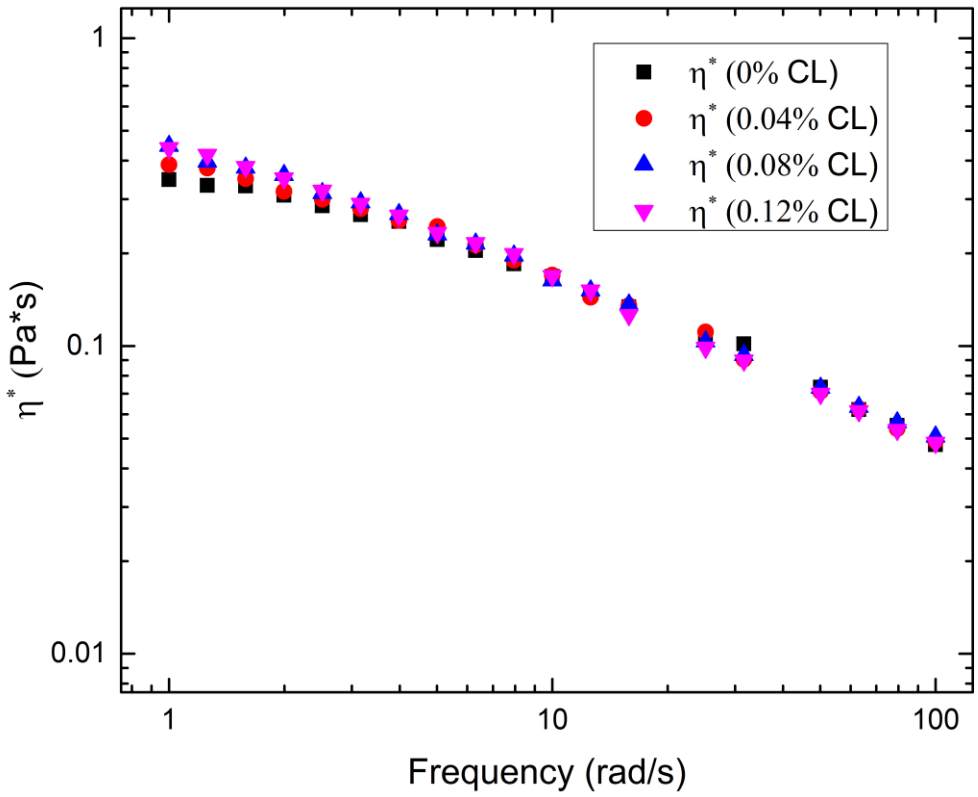

Figure 9: Complex viscosity as a function of frequency and CL concentration

Following the dynamic oscillatory experiments, steady shear flow sweeps were performed to determine the shear viscosity as a function of shear rate. Figure 10, below, depicts the experimental data for this set of experiments.

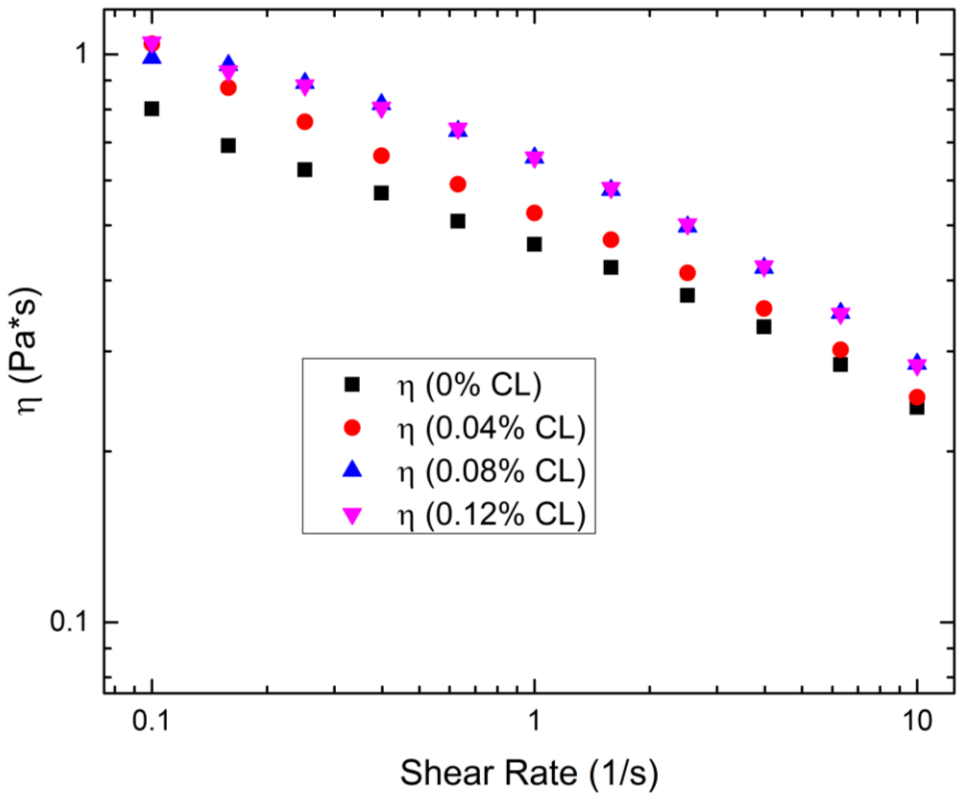

Figure 10: Shear viscosity vs shear rate

4.2 Types of fiber

Different types of chopped fiber are explored for their ability to reduce particle settling rate. The fiber used are summarized in Table 2, shown below.

Table 2 Types of Fiber Used

Fiber	diameter(mm)	length(mm)	Density(g/cm3)
Multimesh Nylon Fiber	0.038	6	1.15
Polyproplyene	0.025	4	0.92
Glass	0.05	6	2.6
Glass	0.05	3	2.6

To compare among types of fiber, the number of fiber per unit volume is kept the same. Mass of an individual fiber is calculated from the fiber's dimension and density, assuming the fiber is a cylinder. The total mass is calculated by multiplying the number of fiber and the mass of one single fiber, which is measurable with an analytical balance. Plots of settling rates vs fiber concentrations for different types of fiber are shown below in Figure 11through Figure 12.

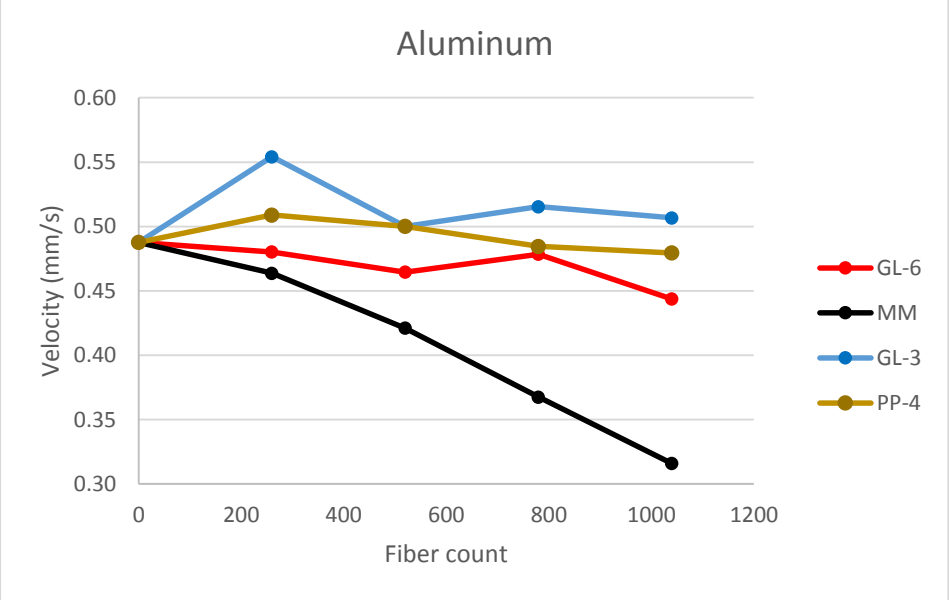

Figure 11: Settling velocity experimental data: Al sphere

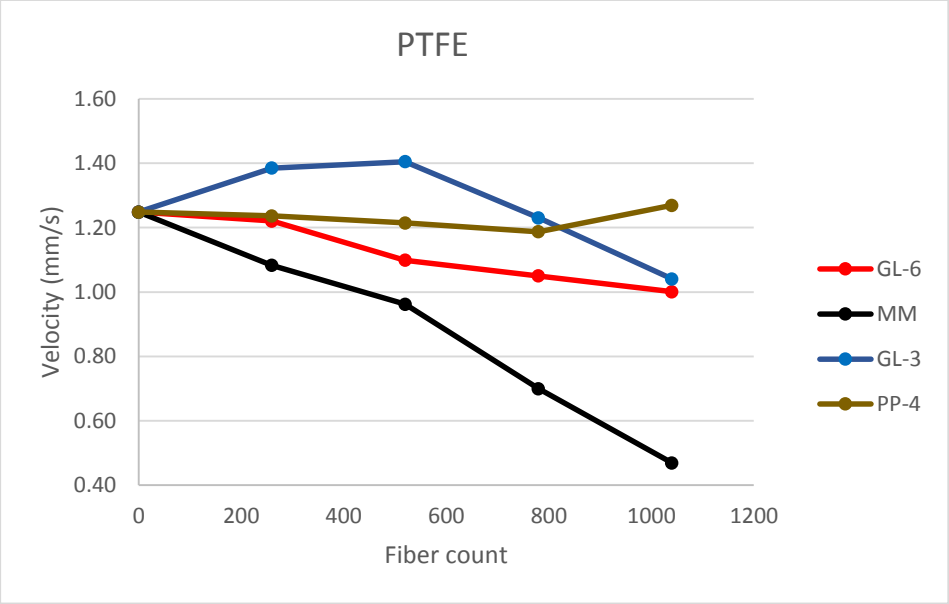

Figure 12: Settling velocity experimental data: PTFE sphere

It is shown that the Multimesh nylon fiber is the most efficient in reducing settling rate.

4.3 A Full Factorial Experiment

Following preliminary experiments, a full factorial experiment exploring cross linker concentration and fiber concentration was performed, measuring settling velocity of four particles in the fluids. Each point in the design space was conducted twice, with the average of the two being shown. Figure 14 through Figure 17, below, illustrates the settling velocity experiments. A master graph of Reynold's number versus drag coefficient is shown in Figure 13.

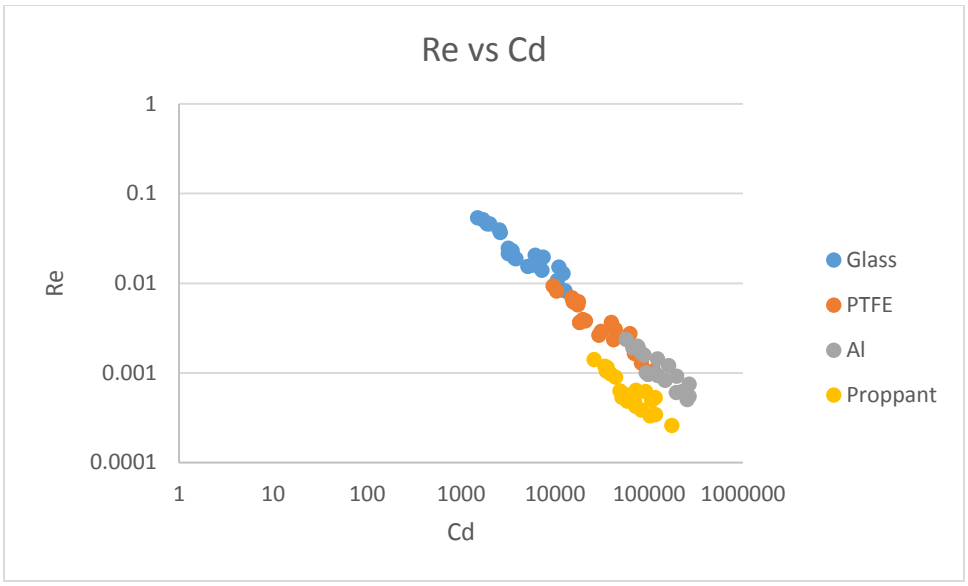

Figure 13: Master graph of experimental data, Reynold's number vs drag coefficient

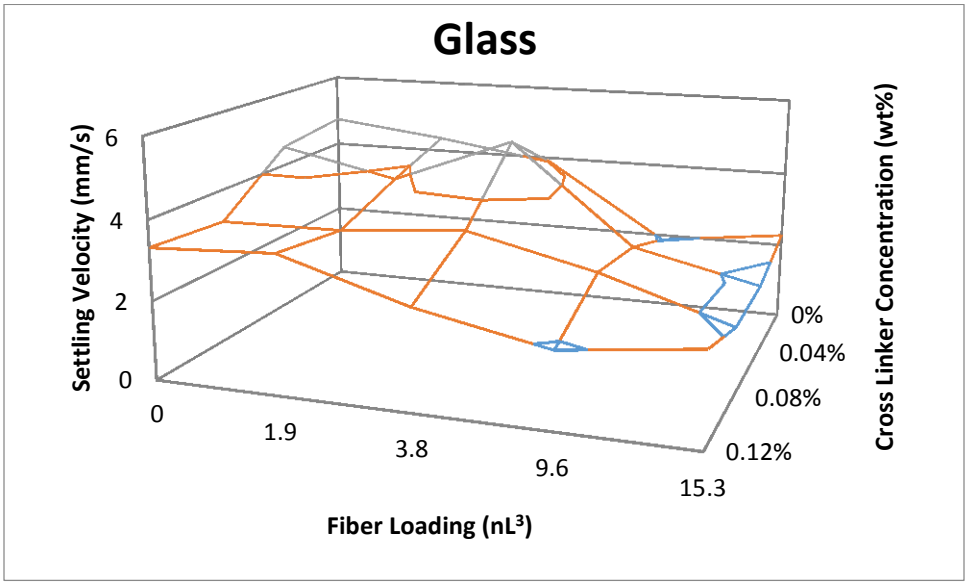

Figure 14: Settling velocity experimental data: Glass sphere

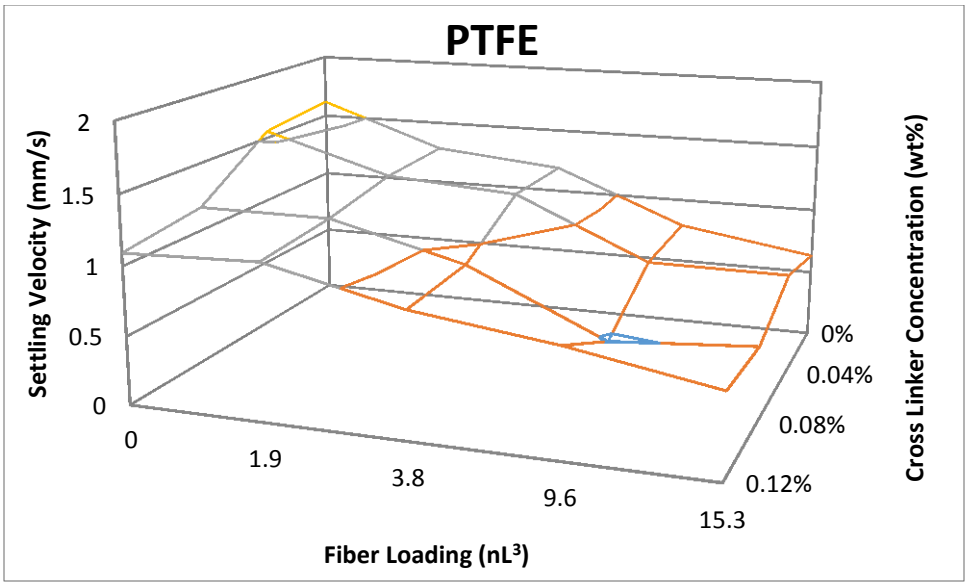

Figure 15: Settling velocity experimental data: PTFE sphere

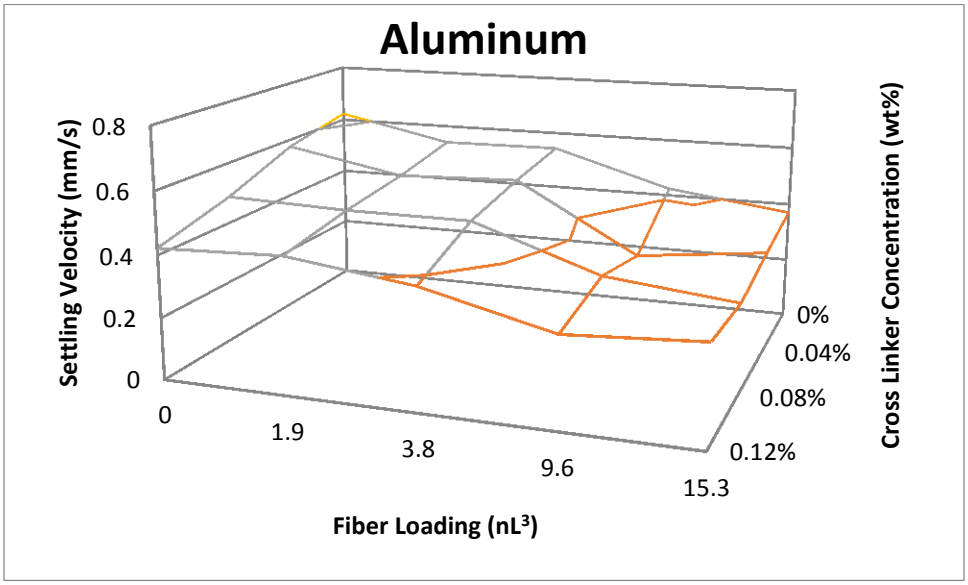

Figure 16: Settling velocity experimental data: Aluminum sphere

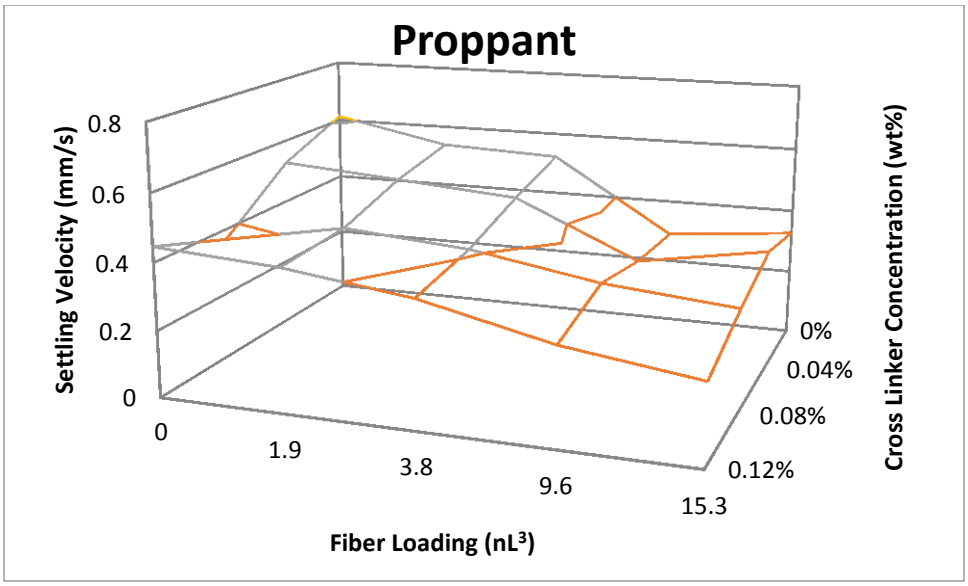

Figure 17: Settling velocity experimental data: Proppant particle

As shown in Figure 18 through Figure 21 below, experimental results indicate that fiber significantly reduces settling rates. At the highest fiber concentration in this research, settling rates are reduced by more than 50%.

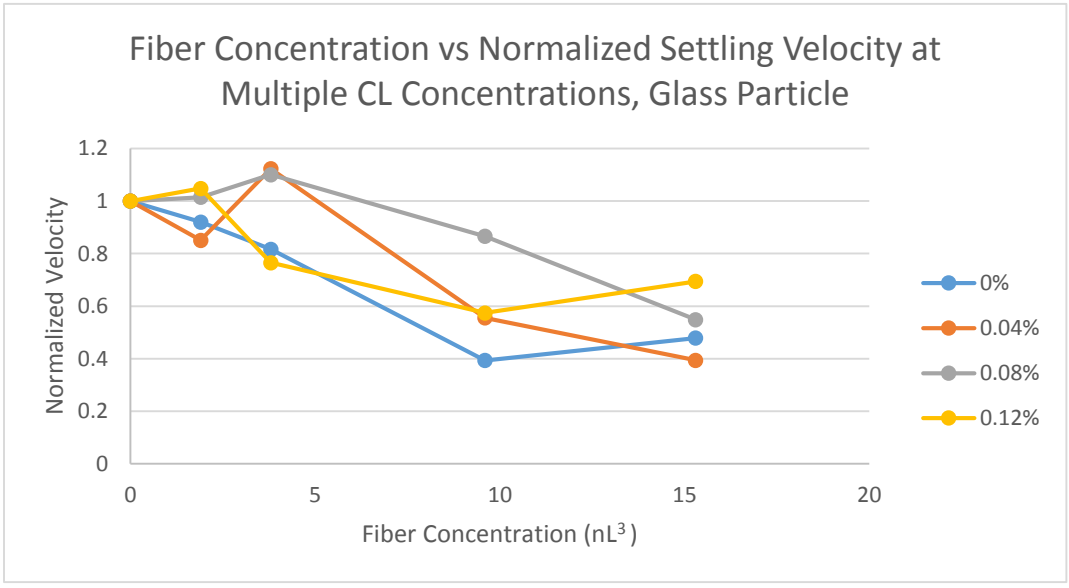

Figure 18 Normalized settling velocity of glass sphere vs fiber concentration

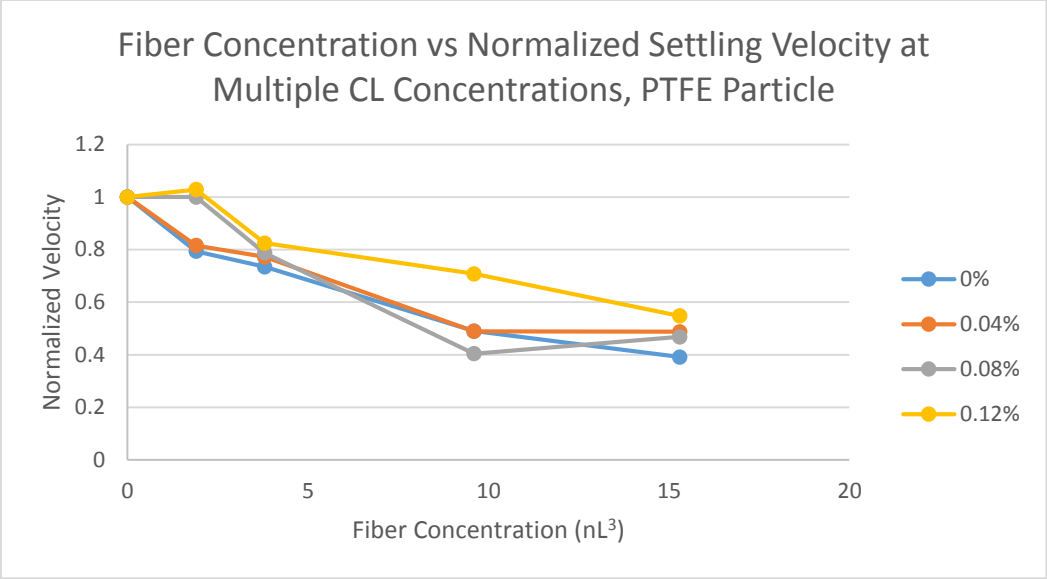

Figure 19 Normalized settling velocity of PTFE sphere vs fiber concentration

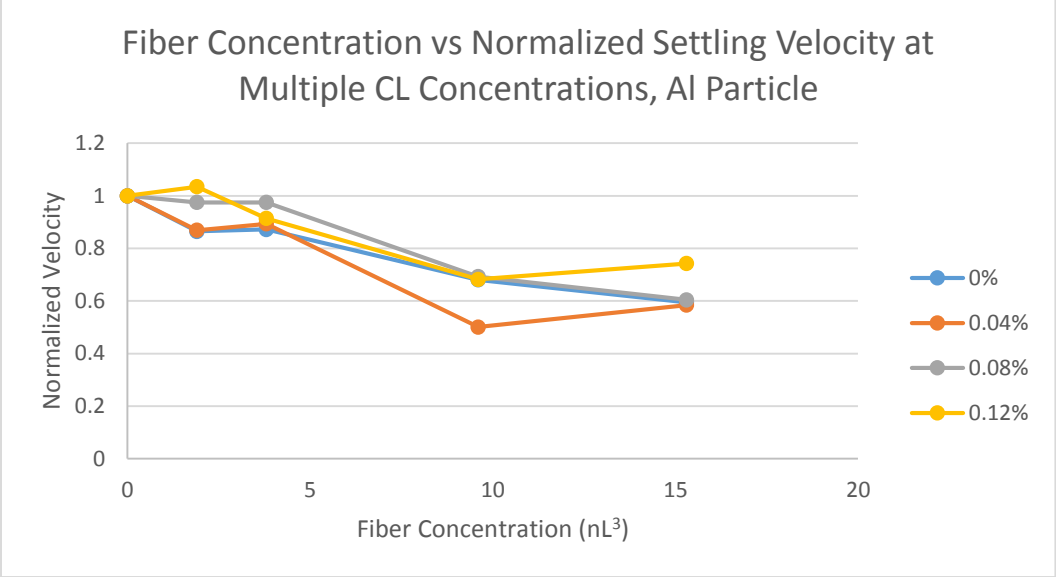

Figure 20 Normalized settling velocity of Al sphere vs fiber concentration

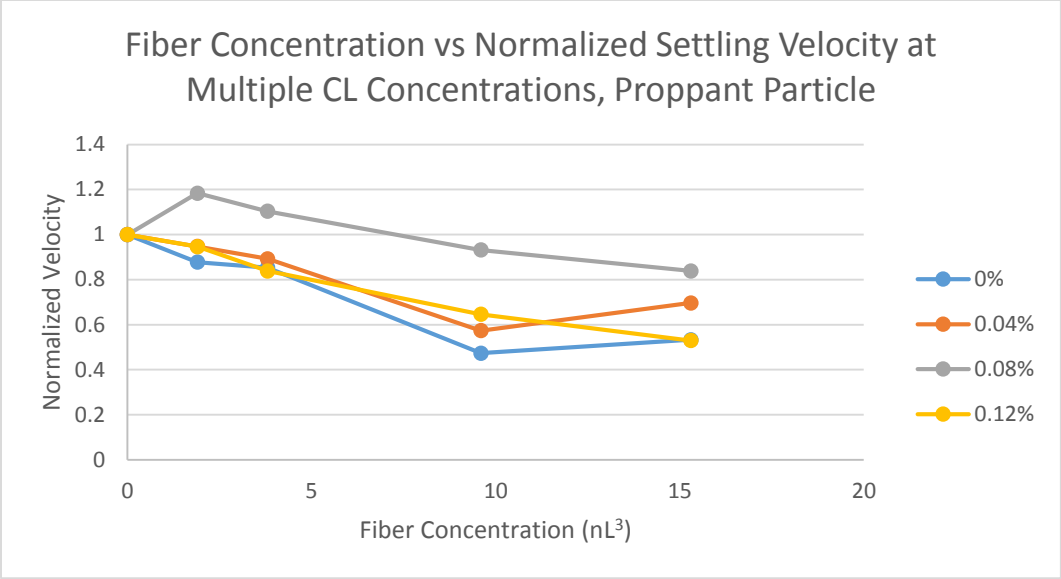

Figure 21 Normalized settling velocity of proppants vs fiber concentration

5. Modeling and Simulation

Three different approaches are used to model the settling behavior of spherical particles in fracking fluids. Stoke's law of settling, empirical correlations in literature and COMSOL simulations.

5.1 Stoke's Law

Stoke's law of settling is the simplest relevant model. It predicts terminal settling rates of a sphere falling through a sea of Newtonian fluid in creep flow region. The terminal velocity is calculated in Equation (1)[6].

$$v_s = \frac{2}{9} * \frac{(\rho_p - \rho_f)}{\eta_0} * gR^2 \qquad (1)$$

For the purpose of calculating settling velocities in a shear-thinning fluid, the Stoke's law equation is solved along with the power law model, shown in Equation (2) and Stoke's maximum shear rate equation, shown in Equation (10)[6][7].

$$\eta_0 = k * \dot{\gamma}^{n-1} \qquad (2)$$

$$\dot{\gamma}_{max} = \frac{3}{2} * \frac{v_s}{R} \qquad (10)$$

In Equation (2), η_0 is the viscosity of the bulk fluid, $\dot{\gamma}$ is the shear rate, k and n are power-law parameters. In Equation (10), $\dot{\gamma}_{max}$ is the maximum shear rate around a sphere. vs is the settling velocity and R is the radius of the sphere.

Solving Equations (1),(2) and (10) together, the terminal settling velocity is expressed in Equation (11) below.

$$v_s = \left[\frac{2 * (\rho_p - \rho_f) * g * R^2}{9 * k * (\frac{3}{2 * R})^{n-1}}\right]^{\frac{1}{n}} \quad (11)$$

In Equation (11), the settling velocity is a function of fluid-particle density difference (ρ_p-ρ_f), gravity g, particle diameter R and power law parameters k and n.

To obtain the power law parameters, The ranges to fit the power law were selected based on the estimated shear rate at the surface of the particle. Maximum shear rates of the spheres used in the experiments are calculated using Equation (10). The results are summarized in Table 3.

Table 3: Shear Rate ranges

	Max Settling Velocity (mm/s)	Shear Rate (1/s)	Min Settling Velocity (mm/s)	Shear Rate (1/s)
Glass	5.06	6.33	1.78	2.22
PTFE	1.62	3.04	0.47	0.89
Aluminum	0.62	1.87	0.29	0.86
Proppant	0.61	2.45	0.29	1.16

With these shear rates in mind, the shear viscosity data were fit using a power law model between shear rates of about 0.5/s to 10/s. The viscosity data modeled is the case with no fiber, since it was previously demonstrated that adding fiber does not significantly affect the viscosity. Figure 22, shown below, illustrates the power law fits to the data, with points representing experimental data and solid lines representing the power law fit. Table 4, also shown below, gives the power law constants fit to the shear viscosity data.

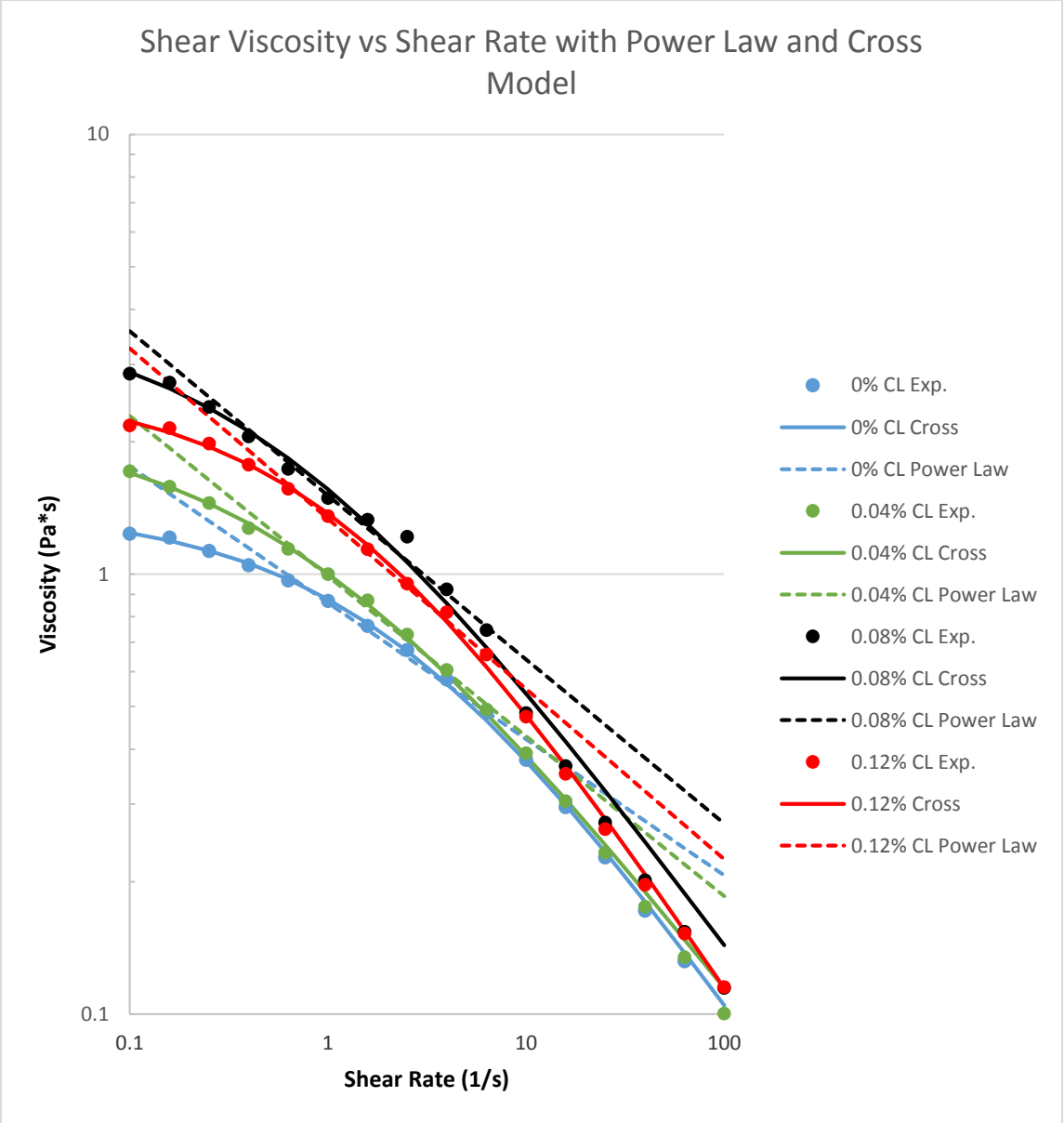

Figure 22: Power Law and Cross Model Fit to Shear Viscosity Data

Table 4: Power Law fitting parameters

	0% CL	0.04% CL	0.08% CL	0.12% CL
k	0.861	0.990	1.511	1.337

n	0.690	0.636	0.627	0.613

Plugging the data into Equation (11), the terminal settling velocity can be calculated. Figure 23 through Figure 26, below, show the Stoke's law prediction for settling velocity.

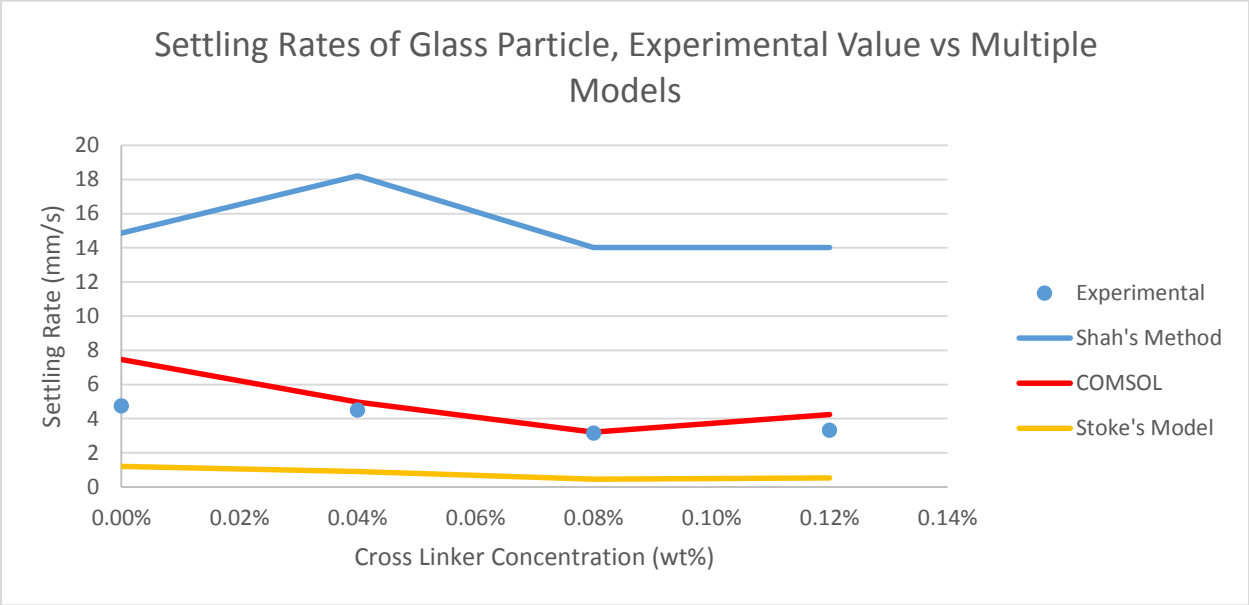

Figure 23: Settling velocity of glass sphere, Stoke's law prediction

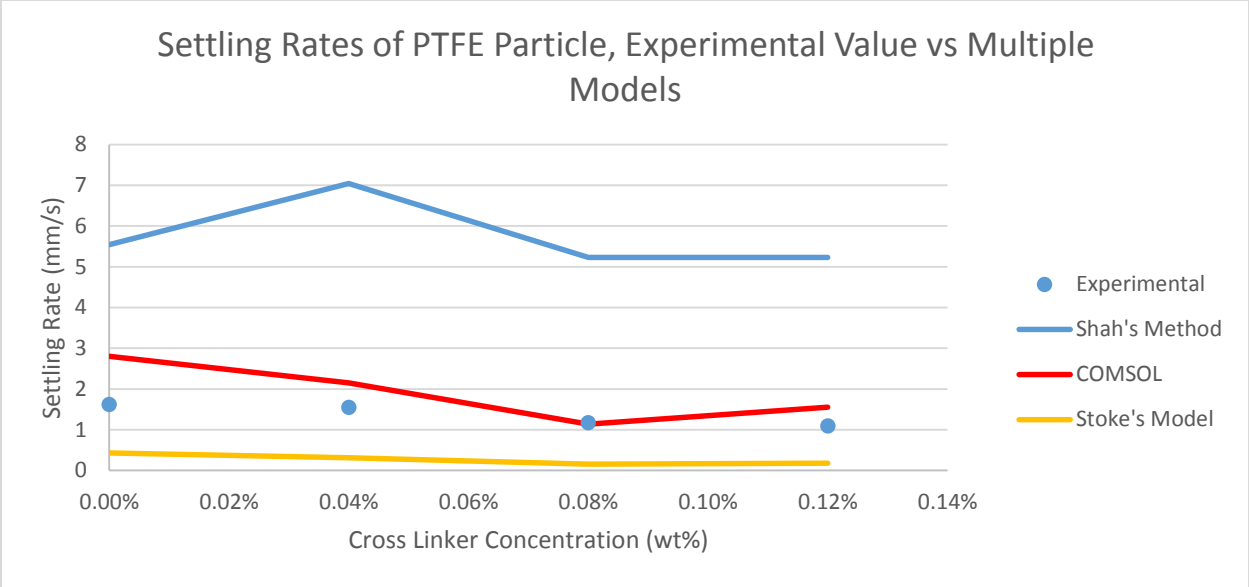

Figure 24: Settling velocity of PTFE sphere, Stoke's law prediction

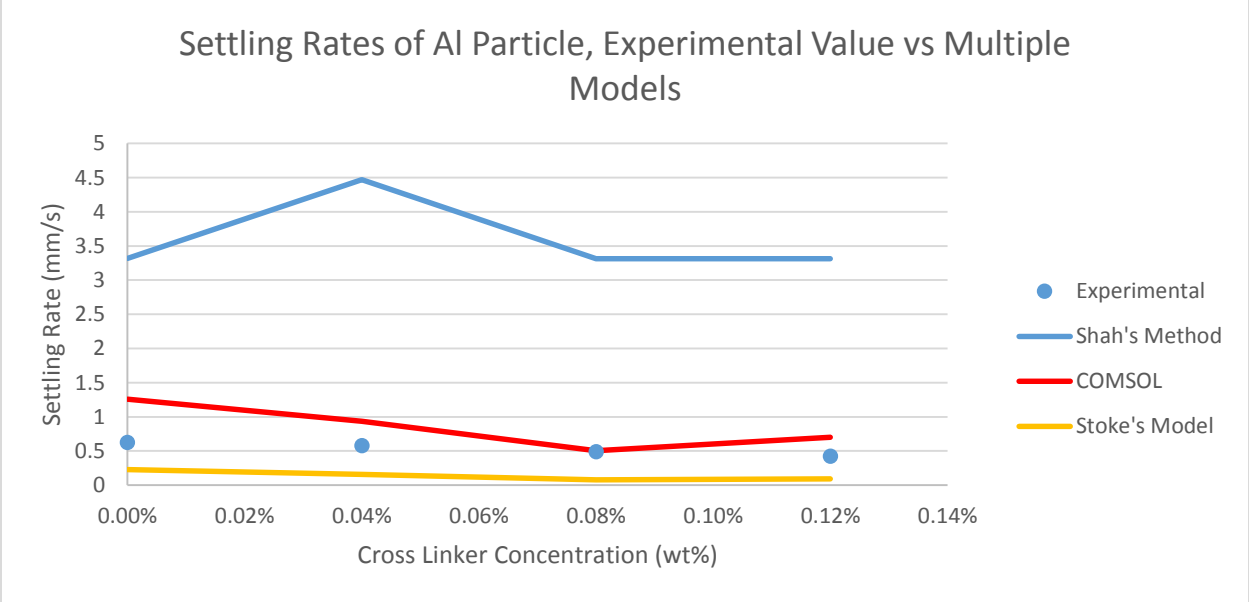

Figure 25: Settling velocity of aluminum sphere, Stoke's law prediction

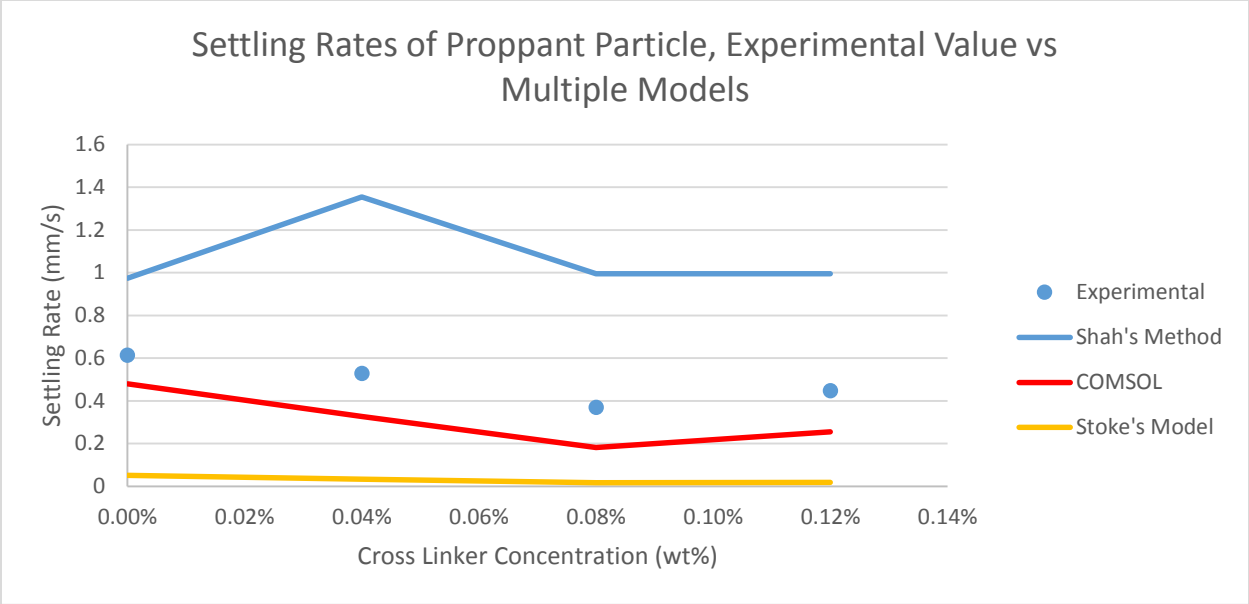

Figure 26: Settling velocity of proppant particle, Stoke's law prediction

As can be seen in the figures, Stoke's law does a poor job of predicting the settling velocity of spherical particles settling in guar gel. In all cases, Stoke's law predicts a significantly lower settling velocity than what is actually observed.

5.2 Empirical Relations

A more sophisticated model proposed by Shah et al [13] relies on the power law model to predict settling of a sphere. As discussed in the literature review section, by multiplying the drag coefficient and Reynold's number such that the settling velocity cancels, the settling velocity of a particle can be predicted empirically with just the power law parameters and the sphere properties. Figure 23 through Figure 26 above show the results of this method.

As can be seen in the figures, the model predicts a much higher settling velocity than what is observed, and overall does a poorer job of predicting settling velocity compared to the Stoke's law approach. The method improves somewhat in accuracy with

the smaller particle size, indicating the method may be useful for rough estimations in hydraulic fracturing applications.

5.3 COMSOL Simulations

Last, sphere settling in a polymer gel was simulated using the COMSOL Multiphysics software. The computational simulation approach allows a more complex rheology model to fit the data across a larger shear rate range to be used to calculate the settling velocity. Through fitting attempts of the rheology data, the fluid is best fitted with Cross Model[7], shown below in Equation (12).

$$\frac{\eta - \eta_\infty}{\eta_0 - \eta_\infty} = \frac{1}{1 + \frac{1}{(K * \dot{\gamma})^{1-n}}} \qquad (12)$$

In equation (12), η_∞ is the viscosity of the fluid at shear rates of infinity, η_0 is the viscosity of the fluid at shear rates of zero, K and n are Cross Model parameters. Shown in Figure 22, Cross Model predicts the rheology of the fluid well, especially when shear rate is lower than 10/s. The Cross Model fitting parameters are summarized in Table 5 below.

Table 5 Cross Model Fitting Parameters

0% CL		0.04% CL		0.08% CL		0.12% CL	
η_0	1.402649	η_0	2.235414	η_0	3.913724	η_0	2.642589
η_∞	0.001	η_∞	0.001	η_∞	0.001	η_∞	0.001
n	0.339942	n	0.409469	n	0.378119	n	0.308923
K	0.460187	K	1.421249	K	1.943019	K	0.890283

A simulation is created in COMSOL Multiphysics. Due to the nature of the software, the simulation approaches the settling process in a slight different way. As shown in Figure 27 below, a fixed geometry is drawn in a 2D Axis-symmetrical plane. The rectangle region is defined as the laminar flow region. The semi-sphere located at the axis of symmetry is the settling spherical particle. Fluid inlet is set at the bottom of the domain. The inlet condition is set to be laminar inflow velocity. The top of the domain is set as open boundary where normal force is set to 0. The side wall is defined as slip condition. The Cross Model parameters are input into the fluid property. A hydraulic force integration is performed on the boundary of the semi-sphere to obtain the total force exerted by the fluid onto the sphere surface. Different inflow velocities are input manually. COMSOL uses steady state momentum balance equations (Equation (13)) and continuity equations (Equation (14)) to numerically solve the problem.

$$\rho(\boldsymbol{u}\cdot\nabla)\boldsymbol{u} = \nabla\cdot[-p\boldsymbol{I} + \mu(\nabla\boldsymbol{u} + (\nabla\boldsymbol{u})^T] + \boldsymbol{F} \quad (13)$$

$$\rho\nabla\cdot(\boldsymbol{u}) = 0 \quad (14)$$

In these two equations, **u** is the velocity vector, p is pressure, I is the identity matrix, μ is the viscosity, **F** is the external force.

The hydraulic force is plotted against the velocity of the fluid and is compared to the gravity exerted on the sphere. The terminal settling velocity is determined by balancing the gravity and the hydraulic force.

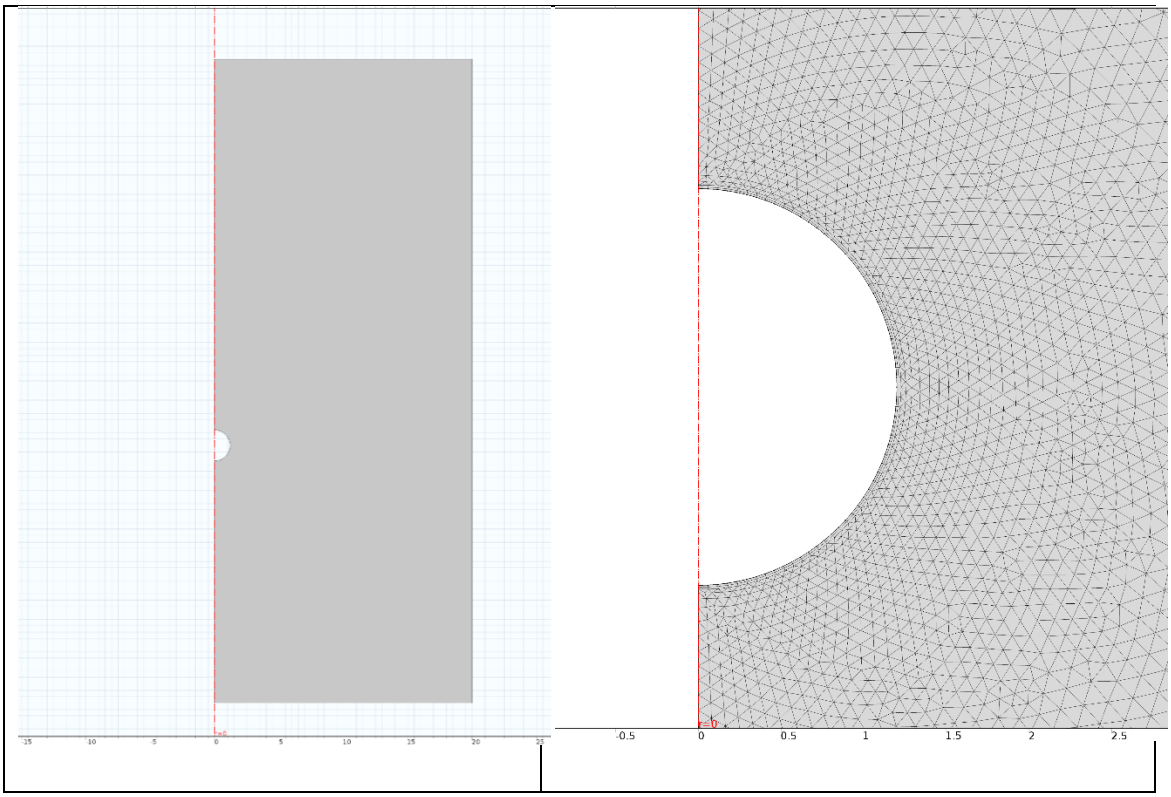

Figure 27 Geometry Setup and mesh in COMSOL Multiphysics

The simulation outputs a variety of information including velocity magnitude and shear rate, shown below in Figure 28 and Figure 29. The terminal settling velocity and shear rate predicted by COMSOL Multiphysics are summarized in Figure 23 through Figure 26 above and Table 6 below.

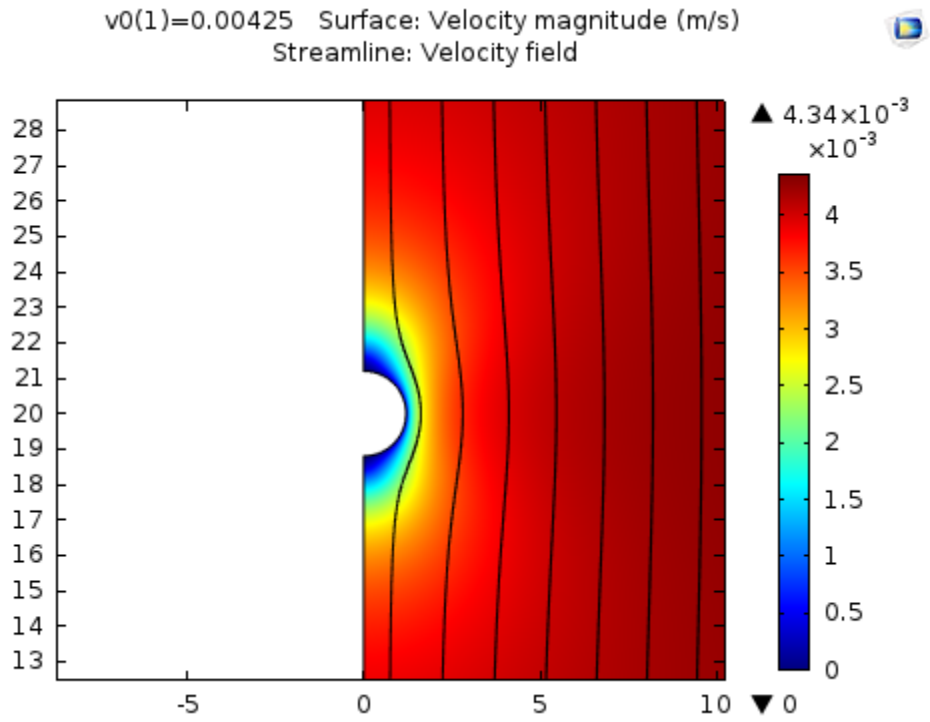

Figure 28 COMSOL Simulation Result, Velocity Magnitude

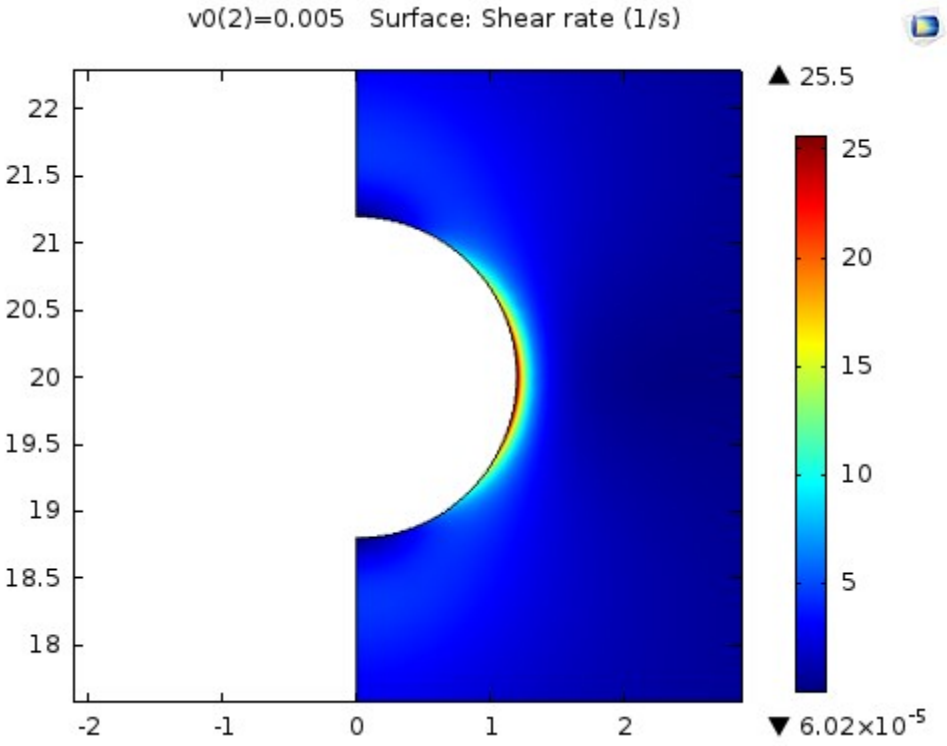

Figure 29 COMSOL Simulation Result, Shear Rate

Table 6 Maximum and Average Shear Rates at Surfaces of Spheres, COMSOL Prediction

	Max Shear Rate (1/s)	Avg Shear Rate (1/s)
Glass		
0% CL	30.292	15.047
0.04% CL	21.537	10.561
0.08% CL	14.812	7.1529
0.12% CL	19.99	9.5926
PTFE		
0% CL	12.189	6.5023
0.04% CL	11.548	5.9196
0.08% CL	5.8594	3.0273
0.12% CL	7.498	3.9044
Aluminum		
0% CL	6.9216	3.8304
0.04% CL	6.4424	3.4113
0.08% CL	3.2622	1.7462
0.12% CL	4.1694	2.2642
Proppant		
0% CL	2.6118	1.537
0.04% CL	2.1181	1.2008
0.08% CL	1.1072	0.6352

0.12% CL	1.432	0.83681

As can be seen in the figures, the COMSOL simulation is more accurate than the previous two models and is not consistently over predicting or under predicting settling velocity than what is experimentally observed. The simulation is superior because Cross Model, a model with more fitting parameters are used to better characterize the rheological property. Also, the simulation is not subject to any empirical relations that might be inaccurate.

5.4 Using COMSOL to model Fiber Effect

As discussed earlier, the addition of fiber does not significantly alter the rheological properties of the fluid medium. Therefore, the aforementioned three modeling methods are unable to predict the effect of fiber on settling rates. Because the inputs to the models are only physical properties of the particles and the rheological properties of the fluid.

To capture the effect of fiber on particle settling rate, a 2D time dependent fluid structure interaction module is built in COMSOL. As shown in Figure 30 below, the model consists of a spherical particle with diameter of 0.5mm settling in a block of fluid. The top boundary is specified to be the inlet with an inflow velocity of 0 m/s. The bottom boundary is specified to be the outlet with pressure specified to be 0 Pa. The two side walls are set to be perfectly slip. The fluid is set to be a Newtonian fluid with density of 1000 kg/m^3 and viscosity of 1 Pa*s. The sphere is specified to be aluminum in COMSOL's material library. Gravity is specified as a volume force on the -y direction on both the fluid and the particle. COMSOL uses time dependent momentum balance equations for the fluid (Equation (15)) and continuity equations for the fluid (Equation (16)) and time dependent momentum balance equation (Equation (17)) for the solid to numerically solve the problem.

$$\rho \frac{\partial \boldsymbol{u_{fluid}}}{\partial t} + \rho(\boldsymbol{u_{fluid}} \cdot \nabla)\boldsymbol{u_{fluid}} = \nabla \cdot [-p\boldsymbol{I} + \mu\left(\nabla \boldsymbol{u_{fluid}} + (\nabla \boldsymbol{u_{fluid}})^T\right] + \boldsymbol{F} \quad (15)$$

$$\rho \nabla \cdot (\boldsymbol{u_{fluid}}) = 0 \quad (16)$$

$$\rho \frac{\partial^2 \boldsymbol{u}_{solid}}{\partial t^2} - \nabla \cdot \sigma = \boldsymbol{F}_V \quad (17)$$

In these equations, t is time, $\mathbf{u_{fluid}}$ is the fluid velocity vector, **F** is the external force on the fluid, $\mathbf{u_{solid}}$ is the solid velocity vector, σ is the surface tension and $\mathbf{F}_V$ is the external force on the solid. In this case, both **F** and $\mathbf{F}_V$ are gravity.

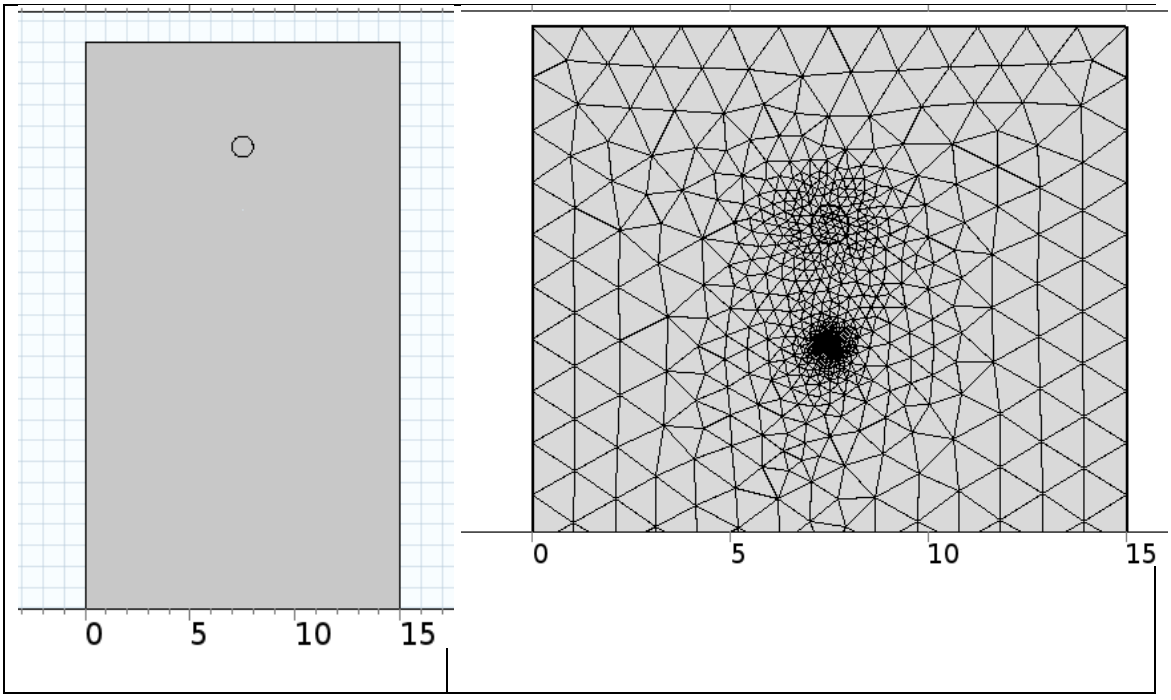

Figure 30 Geometry Setup and mesh in COMSOL Multiphysics

A fiber 0.1mm in diameter is fixed in the geometry. Three fiber-sphere position configuration is computed. The fiber is placed directly below the sphere, one radius off center and 2 radii off center. The simulation results are presented in Figure 31 and Figure 32 below.

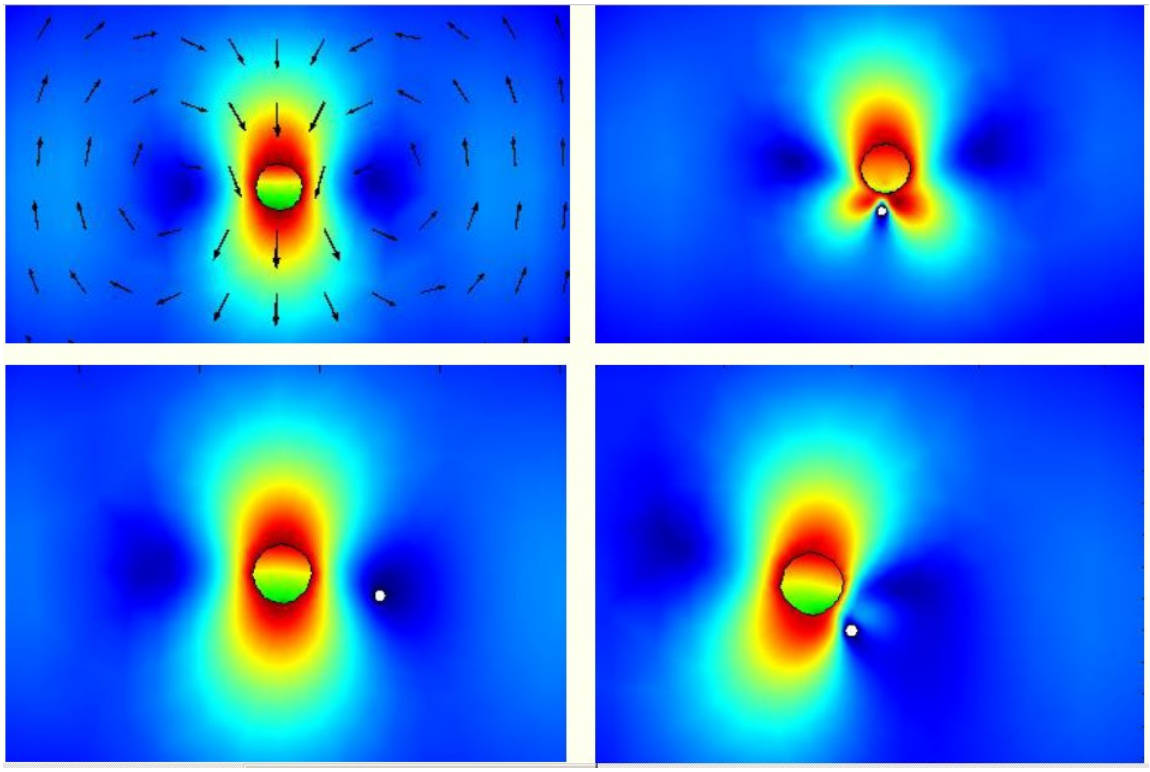

Figure 31 COMSOL Multiphysics simulation results, different fiber configurations

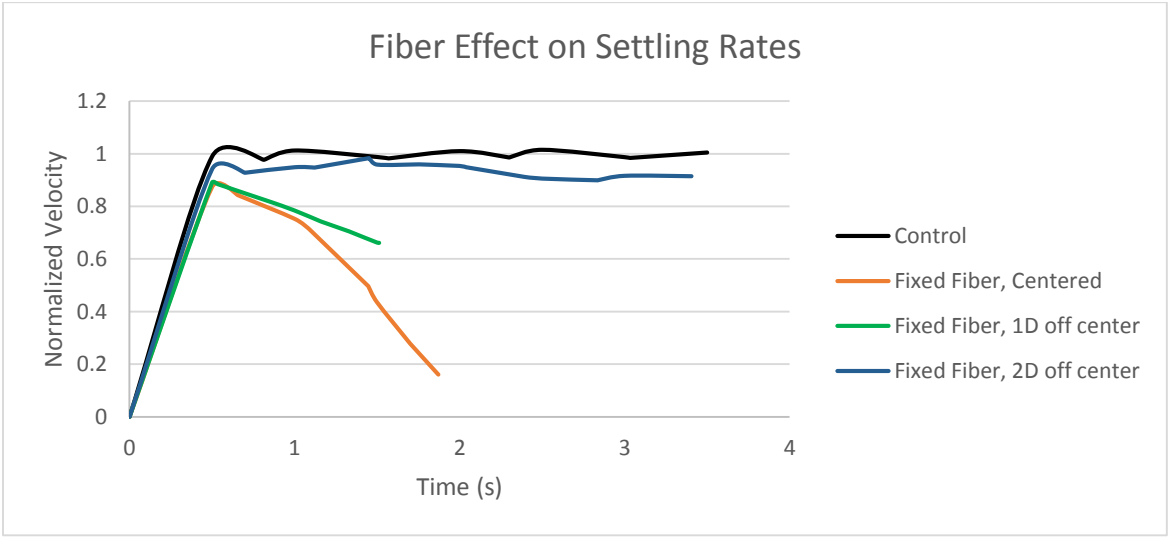

Figure 32 COMSOL Multiphysics simulation results, settling rate

The simulation model is computationally intensive because for every time frame the mesh is stretched. The geometry is remeshed when element distortion passes a certain threshold. As the sphere moves closer to the fiber, mesh elements will distort so much that some of them are inverted within a time step, causing the calculation to fail during the final stages of ascending. As shown in the results, one single fixed fiber directly below the sphere reduces the settling rate by more than 75%. The interaction between the fiber and the sphere decreases significantly as the fiber moves away from the path of the sphere.

The fixed fiber model is not the best model to capture the fiber effect. The model made an assumption that the fiber is perfectly fixed, in which case, if the sphere is settling in a sea of fluid or settling along the axis of symmetry of the well, it should settle onto the fixed fiber and its velocity reduced to 0. This scenario is rarely encountered in experiments because the fiber is floating in the fluid and has elastic properties.

With the mobility of fiber in mind, a floating fiber model is built and computed. In this model, a neutrally buoyant fiber is placed as an object in the fluid. As the sphere settle towards the fiber, the fiber is pushed away from the sphere. The settling velocity results are shown in Figure 33. The sphere and fiber movement results are shown in Figure 34 and Figure 35.

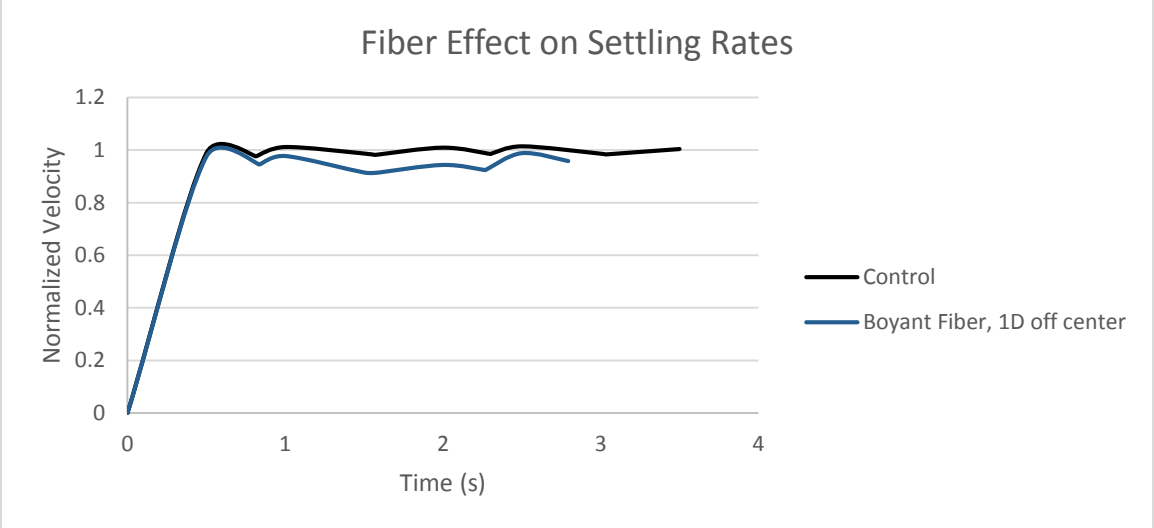

Figure 33 COMSOL Multiphysics simulation results, settling rate

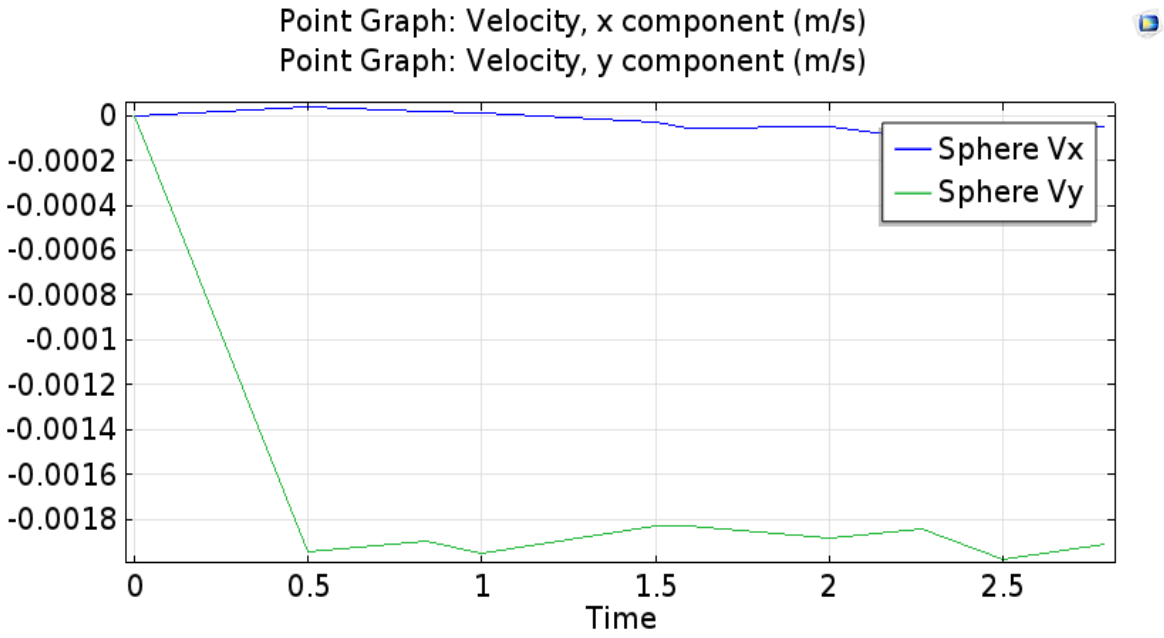

Figure 34 COMSOL Multiphysics simulation results, velocity field of sphere

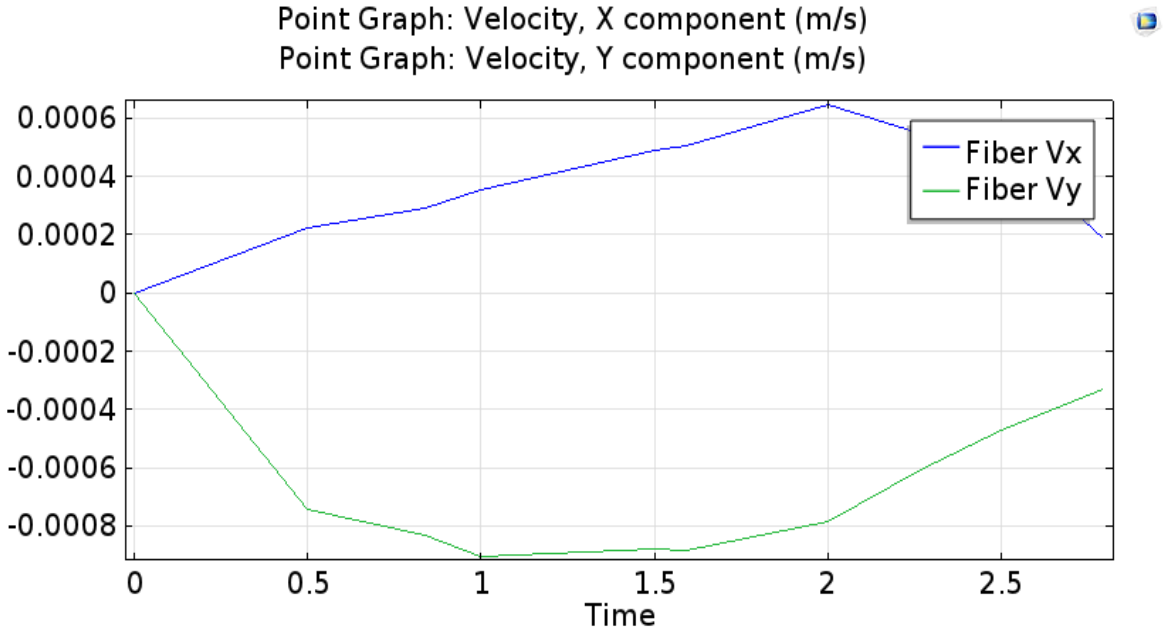

Figure 35 COMSOL Multiphysics simulation results, velocity field of fiber

As shown in the figures, a single floating fiber reduced the sphere settling rate by 10%. The fiber This is smaller velocity reduction is more likely to be observed experimentally. The simulation also has its significance in scaling up. The velocity profiles of a sphere and a fiber can be used as approximation to replace time-dependent brute-force force analysis. This enables a faster calculation when calculating multiple particles settling in a fiber matrix. However, the floating fiber model did not capture the elastic deformation of the fiber.

5.5 Use Sphere-Fiber Interaction Results to Estimate Bulk Behavior

As shown in the previous section, a floating fiber reduces the settling rate of a n interacting sphere by approximately 10%. With this in mind, a scale-up calculation can be performed to estimate the bulk behavior.

Based on the velocity field shown in Figure 28, an effective distance d_{eff} can be estimated to be three times the particle diameter D, as shown in Equation (18).

$$d_{eff} = 3 * D \tag{18}$$

When a particle settles in the fluid, it is safe to assume that it is interacting only with the cylinder of fluid directly beneath itself. Assuming the cylinder has a diameter the same as the sphere and has a length of L and a volume of V. The relationship among the diameter, the length and the volume is shown in Equation (19), below.

$$L = \frac{4V}{\pi * D^2} \tag{19}$$

Define the percent reduction of the particle-fiber interaction as δ, the settling rate as v_s, the reduced settling velocity due to fiber hindering as $v_{s,\,fiber}$, then Equation (20) below holds:

$$v_{s,fiber} = (1 - \delta) * v_s \tag{20}$$

Define effective time t_{eff} as the time the particle interacting with one fiber, the quantity can be approximated in Equation (21) below.

$$t_{eff} = \frac{4V}{\pi * D^2 * v_{s,fiber}} \tag{21}$$

The adjusted overall settling rate v_{adj}, then can be calculated as a weighted average over time, shown in Equation (22) below.

$$v_{adj} = v_{s,fiber} * \frac{n * t_{eff}}{t} + v_s * \frac{t - n * t_{eff}}{t} \quad (22)$$

In this equation, n is the number of fiber the particle is interacting with throughout the settling process.

Plugging in the relations shown above, the adjusted settling rate can be expressed as a function of δ, v_s, D and fiber concentration in number of fibers per volume, n/V, shown in Equation (23), below.

$$v_{adj} = v_s - \frac{\delta}{(1-\delta)} * \frac{3 * \pi * D^3}{4} * \frac{n}{V} \quad (23)$$

This equation depicts the effect caused by fiber, after the settling velocity in fracking fluids without fiber is known, either experimentally or computationally.

By plugging in the data, estimation of macro-scale fiber effect on particle settling rate is summarized in Figure 36 through Figure 39 below

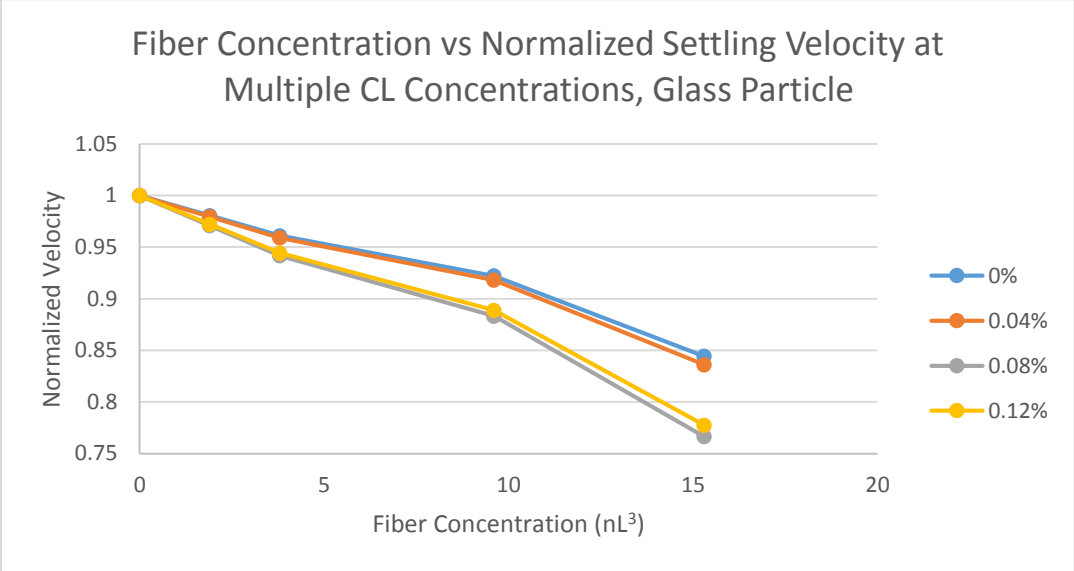

Figure 36 Normalized settling rate of glass vs fiber concentration, model estimation

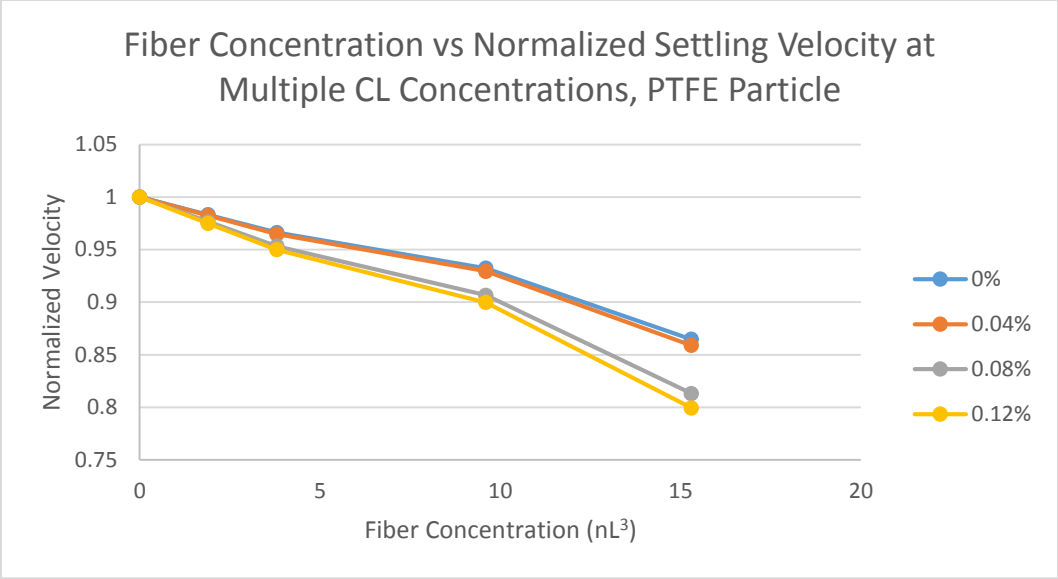

Figure 37 Normalized settling rate of PTFE vs fiber concentration, model estimation

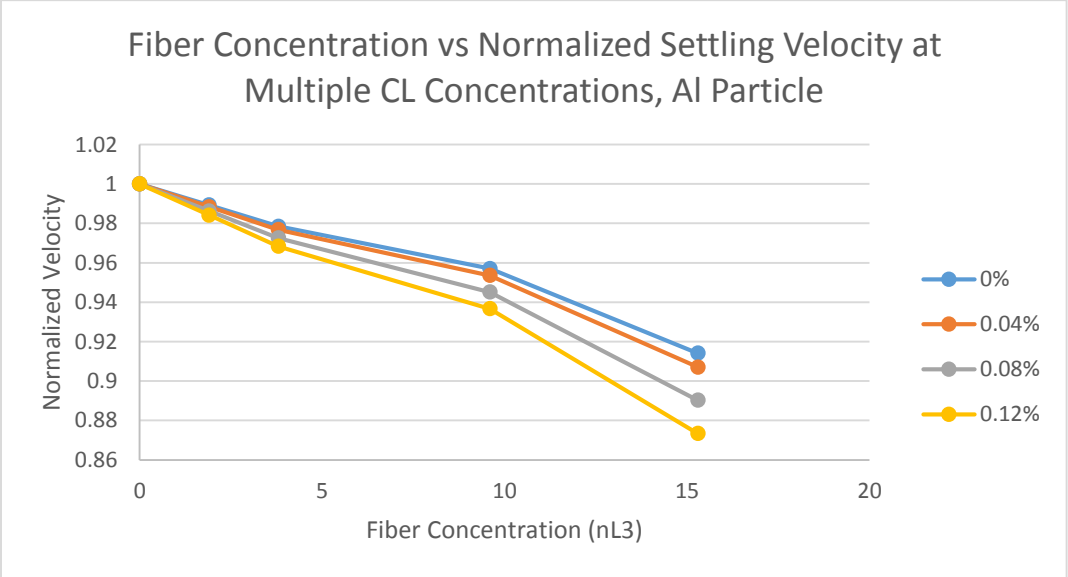

Figure 38 Normalized settling rate of Al vs fiber concentration, model estimation

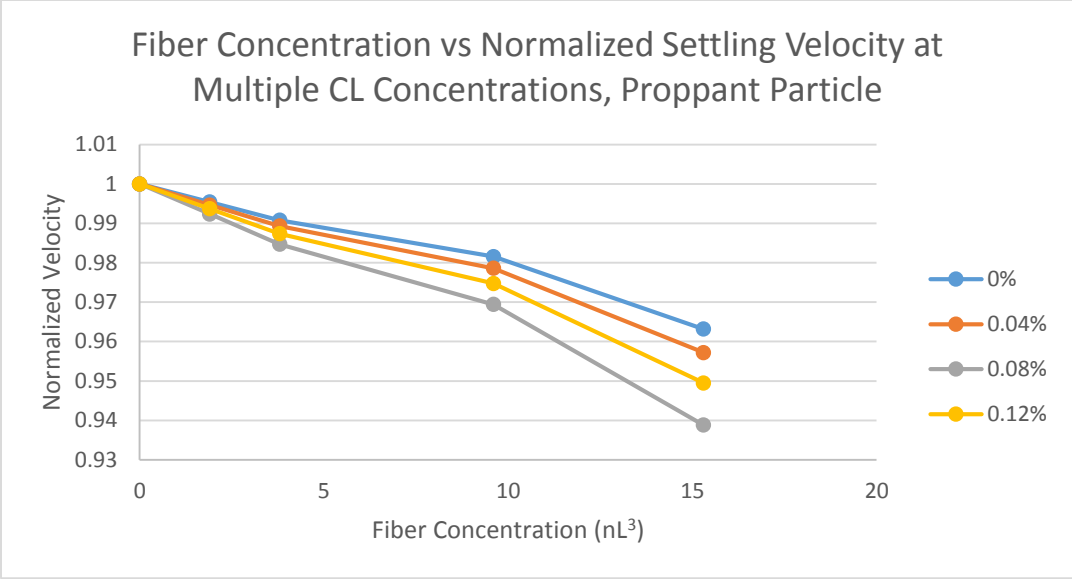

Figure 39 Normalized settling rate of proppant vs fiber concentration, model estimation

As can be seen from the graphs, the model underestimates the effect of fiber. There are two reasons that contributes to this error. First, the simulation is 2-dimensional, meaning the model is most accurately predicting the interactions between two infinitely long cylinders rather than a sphere interacting with a cylinder. Second, the model does not account for the structural deformation, elastic and non-elastic, of the fiber. The model did not account for fiber-fiber interactions either.

6. Conclusions and Future Work

This research investigated settling dynamics of spherical particles in fracking fluid systems. Rheological measurements are conducted to characterize the fluids. For each sample both dynamic oscillatory shear and steady shear measurement are done. Steady shear rate sweep data is fit to Cross Model and is used as inputs for simulation. Settling experiments are done to directly measure the settling rate. The simulation and experimental data are compared against each other.

As demonstrated, Cross Model is a better candidate to characterize fracking fluid than power law model. By using COMSOL, Cross model can be implemented into finite element calculations to better predict settling rates. Results show that COMSOL model is more accurate than Stoke's law and other existing empirical models.

Settling rate experiments with chopped fiber show that fiber has a significant effect in reducing particle settling rate. The result can be directly applied to fracking wells to reduce cross linker usage. For example, the fluid with no cross linker and a fiber loading of 9.6 nL^3, or 0.05 weight % fiber has approximately the same settling velocity as the fluid with 0.08% cross linker and no fiber. Addition of fiber has negligible effect on shear viscosity while higher cross linker concentration has higher viscosity. Therefore the substitution is more environmentally friendly in that less harmful chemical additives are added as well as lower energy cost of pumping is required for a less viscous fluid. The effect of fiber on settling rate is also captured by a simplified COMSOL model.

There is a clear need for a faster and more robust computational fluid dynamics algorithm for computations with moving geometries. COMSOL does not handle moving boundaries well and is very prone to error when the mesh quality drops. There is also a need for the development of constitutive models that can predict the bulk settling velocity of a sphere falling through a fiber-laden aqueous polymer gel, as the models presented

here investigated a single particle interacting with a single fiber in a fluid domain with slip walls. It is impractical to simulate bulk behavior using brute force fluid dynamics computation due to the large number of particles and fiber involved. The bulk simulation also has to take into account particle-particle interaction, fiber-fiber interaction as well as non-isothermal conditions.

7. References

[1] Sovacool, Benjamin K. (09/2014). "Cornucopia or curse? Reviewing the costs and benefits of shale gas hydraulic fracturing (fracking)". *Renewable & sustainable energy reviews (1364-0321)*, 37, p. 249.

[2] Metzner, A. B. "*Rheology of Suspensions in Polymeric Liquids.*" Journal of Rheology 29.6 (1985): 739-75. Print.

[3] Chapin RE, Ku WW. "*The reproductive toxicity of boric acid*." Environ Health Perspect. 1994 Nov;102 (Suppl 7):87–91

[4]OLIVER G. HARLEN, R. R. SUNDARARAJAKUMAR and DONALD L. KOCH (1999). Numerical simulations of a sphere settling through a suspension of neutrally buoyant fibres. Journal of Fluid Mechanics, 388, pp 355-388 doi:10.1017/S0022112099004929

[5] Elgaddafi, Rida (04/2012). "Settling behavior of spherical particles in fiber-containing drilling fluids". *Journal of petroleum science & engineering (0920-4105)*, 84-85, p. 20.

[6] Bird, R.B. (2002). *Transport Phenomena*. John Wiley & Sons, Inc

[7] Macosko, C. W. (1994). *Rheology: Principles, measurements, and applications*. New York: VCH.

[8]Andrić, J. (10/2014). "Rheological properties of dilute suspensions of rigid and flexible fibers". *Journal of non-Newtonian fluid mechanics (0377-0257)*, 212, p. 36.

[9]Tozzi, E. J. (10/2013). "Effect of fiber length, flow rate, and concentration on velocity profiles of cellulosic fiber suspensions". *Acta mechanica (0001-5970)*, 224 (10), p.

[10]"Hydraulic Fracturing at Rosetta." *Hydraulic Fracturing*. N.p., n.d. Web. 19 Feb. 2015.

[11]Al Granberg, "fracking" September 13, 2011 via Flickr, Creative Commons Attribution.

[12] Hercules Incorporated, "Guar and Guar Derivatives Oil and Gas Field Applications," 2007. [Online]. Available: http://www.ashland.com/Ashland/Static/Documents/AAFI/PRO_250-61_Guar.pdf.
[13] "Make Guar Gum Slime (Polymers)," [Online]. Available: http://www.miniscience.com/projects/slime/GuarGumSlime.html. [Accessed April, 1st , 2016].

[14] D.I. Graham, T.E.R. Jones, "Settling and transport of spherical particles in power-law fluids at finite Reynolds number", *Journal of Non-Newtonian Fluid Mechanics,* 54(1994). Pg. 465-488

[15] R. Clift, J. R. Grace, and M. E. Weber, *Bubbles, Drops and Particles* (Academic Press, London, 1978).

[16] Shah, Subhash N, Fadili Y. El, and R.P Chhabra. "New Model for Single Spherical Particle Settling Velocity in Power Law (visco-Inelastic) Fluids." *International Journal of Multiphase Flow*. 33.1 (2007): 51-66. Print.